

1 **Transcript- and annotation-guided genome assembly of the European starling**

2

3 Katarina C. Stuart^{1†}, Richard J. Edwards^{2†}, Yuanyuan Cheng³, Wesley C. Warren⁴, David W.
4 Burt⁵, William B. Sherwin¹, Natalie R. Hofmeister^{6,7}, Scott J. Werner⁸, Gregory F. Ball⁹,
5 Melissa Bateson¹⁰, Matthew C. Brandley¹¹, Katherine L. Buchanan¹², Phillip Cassey¹³, David
6 F. Clayton¹⁴, Tim De Meyer¹⁵, Simone L. Meddle¹⁶, Lee A. Rollins¹

7 ¹ Evolution & Ecology Research Centre, School of Biological, Earth and Environmental
8 Sciences, UNSW Sydney, Sydney, New South Wales, Australia

9 ² School of Biotechnology and Biomolecular Sciences, UNSW Sydney, Sydney, New South
10 Wales, Australia

11 ³ School of Life and Environmental Sciences, The University of Sydney, Sydney, New South
12 Wales, Australia

13 ⁴ Department of Animal Sciences, Institute for Data Science and Informatics, The University
14 of Missouri, Columbia, Missouri, USA

15 ⁵ Office of the Deputy Vice-Chancellor (Research and Innovation), The University of
16 Queensland, Brisbane, Australia

17 ⁶ Department of Ecology and Evolutionary Biology, Cornell University, Ithaca, NY 14850

18 ⁷ Fuller Evolutionary Biology Program, Cornell Lab of Ornithology, Ithaca, NY 14850

19 ⁸ United States Department of Agriculture, Animal and Plant Health Inspection Service,
20 Wildlife Services, National Wildlife Research Center, Fort Collins, Colorado, USA.

21 ⁹ Department of Psychology, University of Maryland, College Park, MD 20742 USA

22 ¹⁰ Institute of Neuroscience, Newcastle University, Newcastle upon Tyne, UK

23 ¹¹ Carnegie Museum of Natural History, Pittsburgh, Pennsylvania, USA

24 ¹² School of Life and Environmental Sciences, Deakin University, Waurn Ponds, VIC, 3228,
25 Australia

26 ¹³ Invasion Science & Wildlife Ecology Lab, University of Adelaide, Adelaide SA 5005,
27 Australia

28 ¹⁴ Department of Genetics & Biochemistry, Clemson University, South Carolina 29634

29 ¹⁵ Dept. of Data Analysis & Mathematical Modelling, Faculty of Bioscience Engineering,
30 Ghent University, Ghent, Belgium

31 ¹⁶ The Roslin Institute, The Royal (Dick) School of Veterinary Studies, The University of
32 Edinburgh, Midlothian, EH25 9RG, UK

33 † Joint first authors

34

35 **Abstract (250 words)**

36 The European starling, *Sturnus vulgaris*, is an ecologically significant, globally invasive avian
37 species that is also suffering from a major decline in its native range. Here, we present the
38 genome assembly and long-read transcriptome of an Australian-sourced European starling (*S.*
39 *vulgaris* vAU), and a second North American genome (*S. vulgaris* vNA), as complementary
40 reference genomes for population genetic and evolutionary characterisation. *S. vulgaris* vAU
41 combined 10x Genomics linked-reads, low-coverage Nanopore sequencing, and PacBio Iso-
42 Seq full-length transcript scaffolding to generate a 1050 Mb assembly on 1,628 scaffolds
43 (72.5 Mb scaffold N50). Species-specific transcript mapping and gene annotation revealed
44 high structural and functional completeness (94.6% BUSCO completeness). Further
45 scaffolding against the high-quality zebra finch (*Taeniopygia guttata*) genome assigned
46 98.6% of the assembly to 32 putative nuclear chromosome scaffolds. Rapid, recent advances
47 in sequencing technologies and bioinformatics software have highlighted the need for
48 evidence-based assessment of assembly decisions on a case-by-case basis. Using *S. vulgaris*
49 vAU, we demonstrate how the multifunctional use of PacBio Iso-Seq transcript data and
50 complementary homology-based annotation of sequential assembly steps (assessed using a
51 new tool, SAAGA) can be used to assess, inform, and validate assembly workflow decisions.
52 We also highlight some counter-intuitive behaviour in traditional BUSCO metrics, and
53 present BUSCOMP, a complementary tool for assembly comparison designed to be robust to
54 differences in assembly size and base-calling quality. Finally, we present a second starling
55 assembly, *S. vulgaris* vNA, to facilitate comparative analysis and global genomic research on
56 this ecologically important species.

57 **Keywords:** *Sturnus vulgaris*, genome assembly, genome assessment, genome annotation,
58 full-length transcripts

59 **Running head:** Genome assembly of the European starling

60

61 **1. Introduction**

62 The European starling (*Sturnus vulgaris*) is a globally invasive passerine that was
63 deliberately introduced during early European acclimatisation efforts into North America,
64 Australia, New Zealand, and South Africa during the mid-late 19th century (Feare 1985).
65 More recently, the species was accidentally introduced into South America (Palacio et al.
66 2016). Since these introductions the invasive ranges of the starling have been expanding, with
67 the species now occupying a range in excess of 38,400,000 km² globally (BirdLife
68 International 2020), posing threats to the economics and health of the agriculture industry, as
69 well as local biodiversity (Bomford & Sinclair 2002; Koch et al., 2009; Palacio et al., 2016;
70 Linz et al., 2017). Recent molecular ecology studies of individuals from the invasive ranges
71 of North America, Australia, and South Africa report that these populations are undergoing
72 rapid and independent evolution in response to novel local selection pressures (Phair et al.,
73 2018; Hofmeister et al., 2019; Bodt et al., 2020; Stuart & Cardilini et al., 2020), a common
74 phenomenon in many invasive populations (Prentis et al., 2008). This suggests the starling has
75 a flexible invasion strategy, potentially enabling colonisation of ecosystems vastly different
76 from those in their native range.

77 Despite their invasive range success, European starlings are increasingly of ecological
78 concern within their native range (Rintala et al., 2003; Robinson et al., 2005). High densities
79 of native range starlings have traditionally been supported by cattle farming across Europe,
80 because starlings preferentially feed in open grasslands, and benefit from invertebrates in

81 overturned soil produced by livestock grazing (Coleman 1977). A shift towards modern
82 indoor cattle rearing processes across Europe may contribute to the decline in starling
83 numbers, which has been a concern since the 1980s (Wretenberg et al., 2006). This decline is
84 reflected globally, with starling and other avifauna numbers decreasing sharply over the last
85 few decades (Spooner et al., 2018; Rosenberg et al., 2019), though this may be further
86 amplified for starling populations subjected to control strategies to reduce their economic
87 impact (Linz et al., 2007). The biological and ecological importance of this species is evident
88 from its prolific use in research, as it is the most studied non-domesticated passerine (Bateson
89 & Feenders 2010). It is evident that future research on the European starling will focus on
90 identifying patterns of evolutionary diversification, and investigating genes associated with
91 invasion success. Such research provides important information for the improvement of
92 control measures and may also provide insight into recovery and dispersive potential in other
93 species that would benefit global conservation efforts. For this, a high-quality, annotated
94 reference genome is essential.

95 Once reliant on large consortia, assembling high-quality reference genomes for
96 genetic analyses is now commonplace. Nevertheless, *de novo* assembly of non-model
97 organism genomes still poses many challenges. Best practices may have not been established
98 for the study species/data, and basic information such as genome size, repeat landscape, and
99 ploidy may be unknown. Furthermore, high-quality references can be generated in multiple
100 ways, which can serve varied research purposes. Rapid developments in both sequencing
101 technology and bioinformatics methods can quickly outdate benchmarking attempts. Whilst
102 not always documented in final publications, the standard practice for non-model species
103 genomes is to select from multiple assemblies generated using different assembly methods,
104 none of which is universally best (Rhie et al., 2020; Whibley et al., 2020). This complexity

105 can be magnified further when sequencing occurs across multiple technology platforms that
106 may be combined and utilised in different ways (Jayakumar & Sakakibara 2019; Kono &
107 Arakawa 2019). The challenge is then to select the best combination of tools and assembly
108 decisions, based on the quality of the genome assemblies produced.

109 A multitude of tools and approaches are available for genome assembly assessment,
110 though some may not be applicable or feasibly implemented for a particular species/assembly
111 and/or the data available (e.g. Bradnam et al., 2013; Hunt et al., 2013; Yuan et al., 2017).

112 Common approaches employed to guide genome assembly decisions focus on contiguity
113 (how continuous the assembled sequences are) and completeness (whether the assembly
114 contains all the genetic information for that species). Two such approaches are assembly
115 statistics (e.g., contig/scaffold counts, and L50/N50 statistics of the number and shortest
116 length of sequences needed to cover 50% of the assembly) and “Benchmarking Universal
117 Single Copy Orthologs” (BUSCO) estimates of genome completeness (Simão et al., 2015).

118 Assembly statistics are very quick to generate and easy to understand, but interpretation can
119 be challenging due to hidden assembly errors and artefacts, which can create false signals.

120 BUSCO assesses the presence or absence of highly conserved lineage-specific genes but is
121 limited to a set of common single-copy genes that may represent easier regions of the genome
122 to sequence and assemble based on current bioinformatics technologies. Furthermore,

123 BUSCO analysis is vulnerable to unpredictable misreporting of presence/completeness for
124 specific genes as a consequence of assembly differences elsewhere in the genome (Edwards et
125 al., 2018; Edwards 2019; Field et al., 2020; Edwards et al., 2021). In addition to the above
126 drawbacks, these methods do not explicitly test the genome assembly’s ability to perform the
127 role for which it was intended (e.g., to serve as a reference genome for specific genomic
128 analysis).

129 Here, we present the first official release of the European starling draft genome, *S.*
130 *vulgaris* vAU. This assembly represents the first synthesis of species-specific full-length
131 transcripts, together with genomic data for this species. In this paper, we complement genome
132 statistics and BUSCO completeness with transcriptome- and annotation-based assessments
133 that help determine genome assembly quality and completeness in the absence of a reference
134 genome to benchmark against. We demonstrate how full-length transcripts can be utilised in
135 genome assembly scaffolding and assessment, in addition to transcriptome construction and
136 annotation. We show how BUSCOMP (<https://github.com/slimsuite/buscomp>) can help avoid
137 over-interpretation or misinterpretation of small differences in BUSCO completeness. We
138 also explore how lightweight homology-based annotation by GEMOMA (Keilwagen et al.,
139 2018), can be used as an assembly assessment using a new tool, SAAGA
140 (<https://github.com/slimsuite/saaga>). Finally, we compare the Australian *S. vulgaris* vAU
141 assembly (GCF_JAGFZL000000000) with an additional (short read) assembly of a North
142 American bird, *S. vulgaris* vNA (GCF_001447265.1), enabling reference-specific biases to be
143 identified in future starling genomics studies.

144

145 **2. Material and Methods**

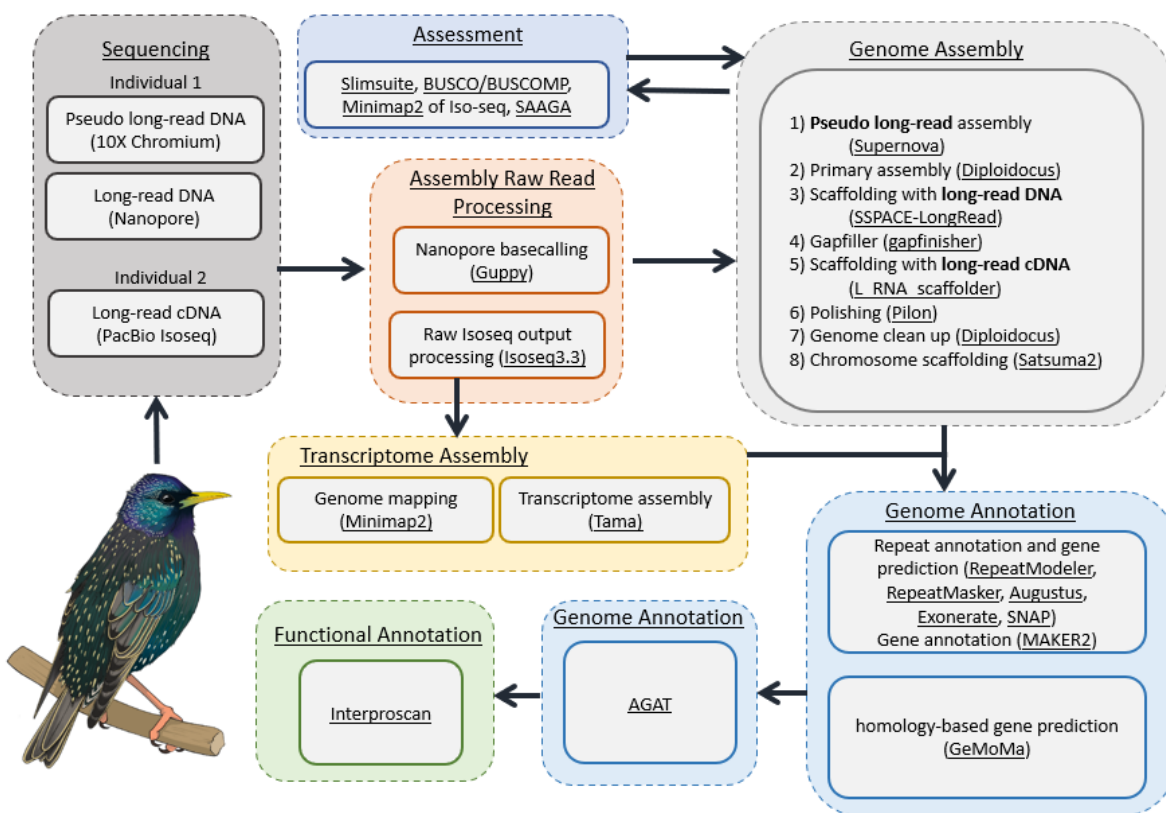
146 **2.1 Genome assembly and scaffolding**

147 The *S. vulgaris* vAU genome assembly used 10x Chromium linked reads and low coverage
148 ONT long reads (Appendix 1: Genomic DNA sample collection, gDNA extraction, and
149 sequencing), and was produced via eight assembly steps (Fig. 1). The 10x reads were
150 assembled into an initial diploid assembly using SUPERNOVA (v2.1.1) (Weisenfeld et al.,
151 2017) with barcode fraction and reads subsample calculated following SUPERNOVA best
152 practices for a genome size based on k-mer counts calculation by JELLYFISH v2.2.10 (Marçais

153 & Kingsford 2011) (parameters: bcfrac = 0.8, maxreads = 550 million, Supplementary
154 Materials: Appendix 2, Validation of SUPERNOVA genome size prediction using JELLYFISH,
155 Supplementary Materials: Fig. S1). This assembly was then split into non-redundant primary
156 and alternative haploid assemblies using DIPLOIDOCUS (parameters: runmode= diphapnr)
157 (v0.9.5) (<https://github.com/slimsuite/diploidocus>). First, both SUPERNOVA pseudohap2
158 assemblies were combined and any sequences lacking definitive base calls (100% Ns) were
159 removed. Remaining scaffolds were size-sorted and gaps reduced in size to a maximum of 10
160 Ns then subject to an all-by-all search with MINIMAP2 (v2.17) (Li 2018) (--cs -p 0.0001 -x
161 asm20 -N 250). (Note that gap size reduction is used for MINIMAP2 searching only, and the
162 non-redundant pseudodiploid assembly produced has the same gap sizes as generated by
163 SUPERNOVA.). Any sequences that were 100% contained within another sequence were
164 removed. Where two or more scaffolds had an 100% identical sequence, only one was kept.
165 Scaffolds are then matched into haplotig pairs based on their SUPERNOVA names. Where a
166 single haplotig is found, it is assigned as diploid, under the assumption that the two original
167 haplotigs were identical with one removed, and added to the primary assembly. (Note: it is
168 possible that only one parent had this scaffold, e.g., a sex chromosome scaffold or structural
169 variant.). If two haplotigs are identified, the longest is assigned to the primary assembly and
170 the shorter to the alternative assembly. The primary assembly should therefore contain an
171 entire haploid copy of the genome, whilst the alternative assembly contains the subset of
172 scaffolds with heterozygous haplotigs.

173 The primary haploid assembly produced by DIPLOIDOCUS was scaffolded using the
174 filtered ONT reads using the program SSPACE-LONGREAD (v1-1) (Boetzer & Pirovano
175 2014). The filtered ONT reads were then used to gap-fill the assembly using GAPFINISHER
176 (v1.0) (Kammonen et al., 2019). Clustered high-quality Iso-Seq reads (see section 2.2 cDNA

177 analysis) were then used for a secondary round of scaffolding using L_RNA_SCAFFOLDER
178 (Xue et al., 2013). Paired-end 10x linked reads were processed with 10X Genomics LONG
179 RANGER (v2.2) and mapped onto this scaffolded assembly using BWA *mem* before error
180 correction of SNPs and indels using PILON (v1.23) (Walker et al., 2014) (parameters: --diploid
181 –fix all settings). To validate the scaffolds, the assembly was analysed using the BREAK10X
182 toolkit in SCAFF10X (v3.1) (<https://github.com/wtsi-hpag/Scaff10X>). The assembly was
183 further checked for assembly artefacts and contamination using DIPLOIDOCUS (parameters:
184 runmode=purgehaplotig & runmode=vecscren (ref); runmode=DipCycle was tested yet
185 discarded due to over-pruning, see Supplementary Materials: Fig. S2) (v0.9.5). Avian species
186 are characterised by distinctive and constrained karyotypes, generally comprised of
187 approximately 10 macrochromosomes and approximately 30 indistinguishable
188 microchromosomes (Griffin et al., 2007; O'Connor et al., 2019), a pattern to which the *S.*
189 *vulgaris* genome conforms (Calafati & Capanna 1981). Therefore, we aligned our assembly to
190 the chromosome scale assembly of zebra finch (*Taeniopygia guttata*) (NCBI=
191 GCF_008822105.2) (Balakrishnan et al., 2010) using SATSUMA2
192 (<https://github.com/bioinfologics/satsuma2>) to create putative chromosomes assuming
193 orthology. This assembly formed the final updated draft genome we present for the species:
194 *Sturnus vulgaris* vAU.
195



196

197 **Figure 1: Workflow for genome assembly and annotation.** A summary of all the
198 experimental methods used for sequencing, genome assembly, transcriptome assembly,
199 genome annotation, and functional annotation, with programs used underlined.

200

201

202

203

204 **2.2 Transcriptome assembly and analysis**

205 Raw PacBio Iso-Seq whole transcript reads (Appendix 3: Transcriptome sample collection,
206 RNA extraction, and sequencing) were processed using the protocol outlined in SMRT LINK
207 (v9.0) (PacBio, California, United States). Briefly, this involved generating Circular
208 Consensus Sequences (CCS) using CCS (v4.2.0), which were then processed using Lima
209 (v1.11.0) for primer removal and demultiplexing. The reads were further processed (PolyA
210 tail minimum length = 8) and clustered using ISO-SEQ (v3.3). The high-quality clustered Iso-
211 Seq reads were then aligned to the reference genome (see section 2.1 Genome assembly and

212 scaffolding) using minimap2 (v2.17) (Li 2018), before further processing using TAMA
213 collapse (Kuo et al., 2020) (settings -a 100 -z 30 -sj sj_priority -lde 5). Both these steps were
214 assessed using BUSCO (v3.0.2b) (Simão et al., 2015) (parameters: aves lineage,
215 transcriptome mode), alongside a short read transcriptome produced from *S. vulgaris* liver
216 RNA (Richardson et al., 2017), as well as other available avian Iso-Seq transcriptomes
217 (Workman et al., 2018; Yin et al., 2019).

218 **2.3 Genome annotation and functional annotation**

219 Each stage of genome assembly was annotated using GEMOMA v1.7.1 (Keilwagen et al.,
220 2018) using the 26 avian genome annotations available on Ensembl at the time this analysis
221 was conducted (Supplementary Materials, Table S1) and with the high-quality clustered Iso-
222 seq, as RNA evidence. The GEMOMA *GeMoMaPipeline* function was run to complete the full
223 pipeline with a maximum intron size of 200 kb (parameters: tblastn=false
224 GeMoMa.m=200000 GeMoMa.Score=ReAlign AnnotationFinalizer.r=SIMPLE pc=true
225 o=true).

226 The final *S. vulgaris* vAU genome assembly was also annotated with MAKER2 (Holt &
227 Yandell 2011) (BLAST+ v2.9 (Camacho et al., 2009), AUGUSTUS v3.3.2 (Stanke &
228 Morgenstern 2005), EXONERATE v2.2.0 (Gs & E 2005), REPEATMASKER v4.0.7 (Smit et al.,
229 2013), REPEATMODELER v1.0.11 (Flynn et al., 2020), and SNAP v0.15.4 (Korf 2004) using
230 repeat-filtered Swiss-Prot protein sequences (downloaded Aug 2018) (UniProt Consortium
231 2019). A custom AUGUSTUS species database was created by running BUSCO using the
232 Optimization mode Augustus self-training mode (--long), using the aves database for lineage.
233 MAKER2 was run using the recommended protocol, including generation of a repeat library,
234 and with the TAMA-processed Iso-Seq data included as primary species transcript evidence,
235 and the pre-existing short read liver transcript data (Richardson et al., 2017) provided as

236 alternate transcript evidence in the first iteration of the MAKER2 annotation process. We ran
237 MAKER2 for a total of three training runs, using the hidden Markov models (HMMs) produced
238 from SNAP training in each subsequent run. *Ab initio* genes were not retained in the final
239 annotation model to produce high-quality and conservative gene predictions. GEMOMA and
240 MAKER2 annotations for the final *S. vulgaris* vAU assembly were combined using the AGAT
241 *agat_sp_merge_annotations* function to produce the final annotation. Functional annotation
242 of protein-coding genes were generated using INTERPROSCAN 5.25–64.0 (parameters: -dp -
243 goterms -iprlookup -appl TIGRFAM, SFLD, Phobius, SUPERFAMILY, PANTHER,
244 Gene3D, Hamap, ProSiteProfiles, Coils, SMART, CDD, PRINTS, Pro SitePatterns,
245 SignalP_EUK, Pfam, ProDom, MobiDBLite, PIRSF, TMHMM). BLAST was used to annotate
246 predicted genes using all Swiss-Prot proteins (parameters: -evaluate 0.000001 -seg yes -
247 soft_masking true -lcase_masking -max_hsps). Annotation summaries were generated using
248 the AGAT *agat_sp_functional_statistics.pl* script, BEDTOOLS was used to calculate gene
249 coverage statistics. Gene ontology terms were assigned using WEGO v2.0 (Ye et al., 2018).

250 **2.4 Annotation assessment using SAAGA: Summarise, Annotate & Assess Genome**

251 **Annotations**

252 SAAGA (Summarise, Annotate & Assess Genome Annotations) (v0.5.3)
253 (<https://github.com/slimsuite/saaga>) was used to assess annotation quality and compare
254 predicted proteins to the repeat- and transposase-filter Swiss-Prot protein sequences used for
255 MAKER2 annotation (above). SAAGA performs a reciprocal MMseqs2 (Steinegger & Söding
256 2017) search of annotated proteins against a (high-quality) reference proteome, identifying
257 best hits for protein identification and employing coverage ratios between query and hit
258 proteins as a means of annotation assessment to generate summary statistics, including:

- **Protein length ratio.** The length ratio of the annotated proteins versus its top reference hit
- **F1 score.** An annotation consistency metric calculated using the formula:

$$(2 \times \text{PROTCOV} \times \text{REFCOV}) / (\text{PROTCOV} + \text{REFCOV})$$

where PROTCOV is the proportion of the annotated protein covered by its best reference protein hit, and REFCOV is the proportion of the best reference protein hit covered by the annotated protein.

- **Completeness.** The summed percentage coverage of reference proteome.
- **Purity.** The summed percentage reference coverage of the annotated proteome.
- **Homology.** The percentage of annotated genes with any hit in reference.
- **Orthology.** The percentage of annotated genes with reciprocal best hits in reference.
- **Duplicity.** The mean number of annotated genes sharing the same best reference hit.
- **Compression.** The number of unique annotated genes that were the top hit for reference proteins, divided by the total number of reference proteins with a hit.
- **Multiplicity.** The ratio of total number of annotated genes to reference proteins.

274 For protein length ratio and F1 score, values close to 1 means that the query protein closely
275 matches the length of the hit protein, indicating high fidelity of the gene prediction model and
276 underlying assembly. The remaining metrics will be closer to 1 (or 100%) for complete
277 annotations and assemblies without duplications, akin to BUSCO scores. Although the
278 maximum achievable value for these metrics will generally be unknown, comparative values
279 can be used to assess improvement in assembly and/or annotation.

280 SAAGA scores may be used to compare alternate annotations of the same assembly,
281 or to compare alternative assemblies in conjunction with consistent annotation. Low genome
282 contiguity, misassembles, or frameshifting indels will affect the quality of predicted genes,

283 with poorer assemblies reporting more fragmented or truncated genes. This approach has been
284 facilitated by the rapid homology-based gene prediction program GEMOMA, which uses
285 reference genome annotation to predict protein-coding genes in the target genome. The
286 program can be run from one line of code and may be parallelised to run much faster than
287 other annotation software (e.g., MAKER2). The ease of this annotation tool opens the way for
288 conducting annotations for the purpose of assessment on sequential or even competing
289 genome annotation steps. Assessing the quality of protein-coding region predictions will help
290 ensure the final genome assembly can produce a high-quality annotation. Here, we used the
291 repeat-filtered Swiss-Prot database used in annotation, and the *Gallus gallus* reference
292 proteome (UP000000539_9031), to assess predicted protein quality and annotated proteome
293 completeness.

294 **2.5 Genome assembly completeness assessment**

295 Assembly contiguity and completeness was assessed for sequential genome assembly
296 steps of the *S. vulgaris* vAU assembly and compared to existing passerine chromosome level
297 assemblies available on NCBI, including the *S. vulgaris* vNA assembly (Assembly accession
298 GCF_001447265.1, Supplementary Material: Appendix 4, Assembly and annotation of the *S.*
299 *vulgaris* vNA genome version).

300 **2.5.1 BUSCO and BUSCOMP assembly completeness assessment**

301 Genome completeness was estimated using BUSCO (v3.0.2b, genome mode, aves
302 lineage). BUSCO resulted were collated across all assemblies using BUSCOMP v0.10.1
303 (<https://github.com/slimsuite/buscomp>). BUSCOMP collated BUSCO outputs across all
304 genome assembly stages and compiled a maximal non-redundant set of 4727 complete
305 BUSCOs found at single copy in at least one assembly. Compiled BUSCO predicted gene
306 sequences were mapped onto each assembly to be rated with MINIMAP2 v2.17 (Li 2018) and

307 re-scored in terms of completeness, thereby providing a robust and consistent means of
308 assessing comparable completeness across assemblies of the same genome.

309 **2.5.2 PacBio Iso-Seq completeness assessment**

310 The PacBio Iso-Seq reads were mapped on to genome assemblies using MINIMAP2
311 (parameters: -ax splice -uf --secondary=no --splice-flank=no -C5 -O6,24 -B4) (Li 2018) and
312 the number of Iso-Seq transcripts mapping on to each assembly, and their corresponding
313 mapping quality, was calculated.

314 **2.5.3 KAT k-mer completeness assessment**

315 The final genome assembly completeness was assessed by examining the read k-mer
316 frequency distribution with different assembly copy numbers based on the 10x Chromium
317 linked reads using K-MER ANALYSIS TOOLKIT (KAT) v2.4.2 (Mapleson et al., 2017) (30 bp
318 trimmed for R1 reads, and 16 bp trimmed for R2 reads).

319 **2.6 Additional genome statistics**

320 The Iso-Seq and final annotation transcript density, final annotation gene density,
321 global SNP variant density (based on a whole genome data set of 24 individuals from United
322 Kingdom, North America, and Australia, N=8 (Hofmeister *et al.* 2021), and GC-content were
323 calculated in sliding windows of width 1 Mb using BEDTOOLS v 2.27.1 (Quinlan & Hall
324 2010), and plotted across the largest 32 scaffolds in our final genome assembly (representing
325 more than 98% of the total assembly captured on putative chromosomes orthologous to other
326 avian chromosomes) using CIRCLIZE (v 0.4.9) (Gu *et al.*, 2014).

327 **2.7 Genome assembly correction**

328 NCBI VecScreen flagged possible bacterial and adapter contamination in the final *S.*
329 *vulgaris* vAU assembly, which was missed by earlier contamination screening steps. An
330 updated version of DIPLOIDOCUS (runmode vecscreen) was run to mask shorter adapter

331 sequences and flag additional organism contaminates (screenmode=purge vecmask=27). Four
332 related bacterial strains (*Delftia acidovorans* SPH-1, *Acidovorax* sp. JS42, *Alicycliphilus*
333 *denitrificans* K601, *Paraburkholderia xenovorans* LB400) were identified, and so GABLAM
334 v2.30.5 (Davey et al., 2006) was used to search these four genomes against the final
335 assembly, and purge small contigs (<5,000 bp) that contained sequence matches (285 short
336 contigs excluded). For larger scaffolds that contained possible embedded contaminated
337 sequences, the high-quality ONT reads were mapped using Minimap2 over the regions. For
338 those contaminated sites that had Nanopore reads spanning the contaminated region, the
339 sequences were masked, and for those lacking nanopore support, the scaffold was split and/or
340 trimmed to remove the contaminating sequence (seq 4 trimmed, seq 12 and 31 split into
341 chromosome and unplaced scaffold). Finally, gaps of unknown size were standardised to 100
342 bp, and mitochondrial genome insertions into the nuclear genome were assessed using
343 NUMTfinder (<https://github.com/slimsuite/numtfinder>) (Edwards et al., 2021) (none located).
344 This paper primarily analyses *S. vulgaris* vAU1.0 (which we refer to has *S. vulgaris* vAU),
345 while the final NCBI release (accession = JAGFZL000000000) is explicitly referred to as *S.*
346 *vulgaris* vAU1.1 when relevant.

347 **2.8 BUSCO versus BUSCOMP performance benchmarking**

348 BUSCO-containing scaffolds from the DIPLOIDOCUS primary haploid SUPERNOVA
349 assembly of *Sturnus vulgaris* vAU were extracted into a reduced genome ‘pribusco’ assembly
350 for additional BUSCO and BUSCOMP benchmarking (Supplementary Materials: Fig. S3).
351 BUSCO v3.0.2b (Simão et al., 2015) (HMMER v3.2.1 (Wheeler & Eddy 2013), AUGUSTUS
352 v3.3.2 (Stanke & Morgenstern 2005), BLAST+ v2.2.31 blast(Camacho et al., 2009),
353 EMBOSS v6.6.0 (Rice et al., 2000)) was run in genome mode with the aves_odb9 dataset
354 (n=4915) on: the non-redundant pseudodiploid (‘dipnr’), primary (‘pri’) and alternative (‘alt’)

355 assemblies; BUSCO-containing scaffolds from the primary assembly ('pribusco'); a reverse-
356 complemented copy ('revcomp'), combined with 'pribusco' to make a 100% duplicate
357 assembly ('duplicate'); a direct copy ('copy') combined with 'duplicate' to make a triplicated
358 assembly ('triplicate'); three randomly shuffled versions of 'pribusco' ('shuffle1', 'shuffle2',
359 'shuffle3'), added in combination to `pribusco` to generate datasets of increasing assembly
360 size without increasing duplication levels ('2n', '3n' and '4n'); ten straight repeats of the
361 `pribusco` run (`rep0` to `rep9`). All BUSCO results were processed with BUSCOMP v0.11.0
362 (MINIMAP2 v2.17). In addition to the full BUSCOMP analysis of all runs, the following
363 subsets were grouped for analysis (Supplementary File 1, BUSCO v3 BUSCOMP output):

364 • Pseudodip: 'dipnr', 'pri' and 'alt'. (Haploid versus diploid assemblies.)
365 • Core: 'dipnr', 'pri', 'alt', 'pribusco' and 'revcomp'. (Assembly filtering and
366 manipulation.)
367 • Duplication: 'copy', 'duplicate', 'triplicate'. (Duplicating scaffolds.)
368 • Size: 'shuffle1', 'shuffle2', 'shuffle3', '2n', '3n', '4n'. (Increasing assembly size
369 without duplication.)
370 • Replicates: 'rep0' to 'rep9'.

371 The same analysis was repeated with BUSCO v5.0.0 (Simão et al., 2015) (SEPP v4.3.10
372 (Mirarab et al., 2012), BLAST v2.11.0 (Camacho et al., 2009), HMMer v3.3 (Wheeler &
373 Eddy 2013), AUGUSTUS v3.3.2 (Stanke & Morgenstern 2005), PRODIGAL v2.6.3 (Hyatt et
374 al., 2010), METAEUK v20200908 (Levy Karin et al., 2020)) and the aves_odb10 dataset
375 (n=8338).

376 **3. Results**

377 **3.1 *Sturnus vulgaris* vAU genome assembly**

378 Genome assembly of *Sturnus vulgaris* vAU combined three different sequencing
379 technologies for *de novo* genome assembly (10x Genomics linked reads, ONT long reads, and
380 PacBio Iso-Seq full length transcripts) (Table 1), before a predicted reference-based
381 scaffolding to the chromosome level using the high-quality reference assembly of *T. guttata*
382 (NCBI REF: GCF_008822105.2). Approximately 109 Gb (97x coverage) of 10x linked read
383 data (subsampled during assembly to 56x based on the estimated genome size of 1.119 Gb,
384 barcode subsampling of 80%) were assembled with SUPERNOVA (v2.1.1) (Weisenfeld et al.,
385 2017) (step 1) and converted to a primary haploid assembly (step2). We generated
386 approximately 8 Gb of raw genomic reads using an ONT minion, which were reduced to 5 Gb
387 after stringent filtering (Table 1). These data were used to scaffold the genome (step 3) and
388 gap-fill (step 4), reducing the total number of scaffolds from 18,439 to 7,856, increasing the
389 scaffold N50 from 1.76 Mb to 7.12 Mb, and decreasing the scaffold L50 from 146 to 39
390 (Supplementary Materials: Fig. S4). These measures were further improved after Iso-Seq
391 scaffolding (step 5) (7,776 scaffolds, N50 7.12 Mb, and L50 38), followed by Pilon polishing
392 using 10x linked reads (step 6). Finally, following haplotig removal (step 7), chromosomal
393 alignment against the *T. guttata* reference genome (step 8) reduced the final number of
394 scaffolds to 1,628 (N50 72.5 Mb, and L50 5) (Supplementary Materials: Fig. S4), with 98.6%
395 of the assembly assigned to 32 putative nuclear chromosome scaffolds. While no whole
396 mitochondrial genome insertions were found, 27 smaller mitochondrial pseudogenes
397 (NUMTs) were located in *S. vulgaris* vAU1.1, with scaffold 31 (corresponding to the Z
398 chromosome) containing the highest amount (Table S2).

399 **Table 1: Summary of sequencing data** for *Sturnus vulgaris* vAU genome assembly and
400 annotation

Genetic Data	Platform	Library	Library length/Mean Insert Size (kb)	Mean raw Read Length (bp)	Number of Reads	Number of bases (Gb)
--------------	----------	---------	--------------------------------------	---------------------------	-----------------	----------------------

gDNA	Hiseq X Ten	Paired-end 10x Chromium	51.7kb	150	361,950,449	108.58
gDNA	ONT MinION	Ligation	47kb	6,417	1,225,865	7.865
cDNA	PacBio	Iso-Seq	Full transcripts (brain) (2.6 kb)	12,000	20,558,110	38.650
cDNA	PacBio	Iso-Seq	Full transcripts (heart + testes) (2.0 kb)	10,000	18,985,944	29.496

401

402 ***Improvements to genome assembly completeness during scaffolding***

403 Sequential steps of scaffolding, polishing, and quality control (Fig. 1, Supplementary
404 Materials: Fig. S2, Table S3) improved the genome assembly statistics considerably from the
405 initial SUPERNOVA *S. vulgaris* assembly (Supplementary Materials: Fig. S4). BUSCO
406 completeness was approximately 94.6%, which was largely achieved by the initial assembly
407 (92.9%), but somewhat improved over the additional assembly steps (Fig. 2a). The final
408 BUSCO completeness score is comparable to other chromosome-level passerine assemblies
409 on NCBI (Fig. 3a). BUSCO predictions are susceptible to base calling errors and can also
410 fluctuate due to changes elsewhere in the genome assembly (Edwards 2019) (see section 2.8
411 BUSCO versus BUSCOMP performance benchmarking). As a consequence, BUSCO can
412 under-report the true number of complete BUSCO genes in an assembly (Edwards et al.,
413 2018; Field et al., 2020; Edwards et al., 2021). We therefore used BUSCOMP to compile
414 complete BUSCO genes from across all stages of the assembly. Only 70 (1.4%) of the 4,915
415 Aves BUSCO genes were found to be “Missing” from all assembly versions, with 4,764
416 (96.9%) rated “Complete” in at least one stage (Fig 3a, BUSCOMP).

417 The final assembly had the fewest unmapped Iso-Seq reads (Fig. 2b), with the largest
418 improvement seen post gap-filling, followed by chromosome scaffolding. An increase in
419 missing Iso-Seq transcripts was observed after scaffolding with the Iso-Seq reads themselves,
420 and post long-read scaffolding, due to reads no longer partially matching at scaffold ends.

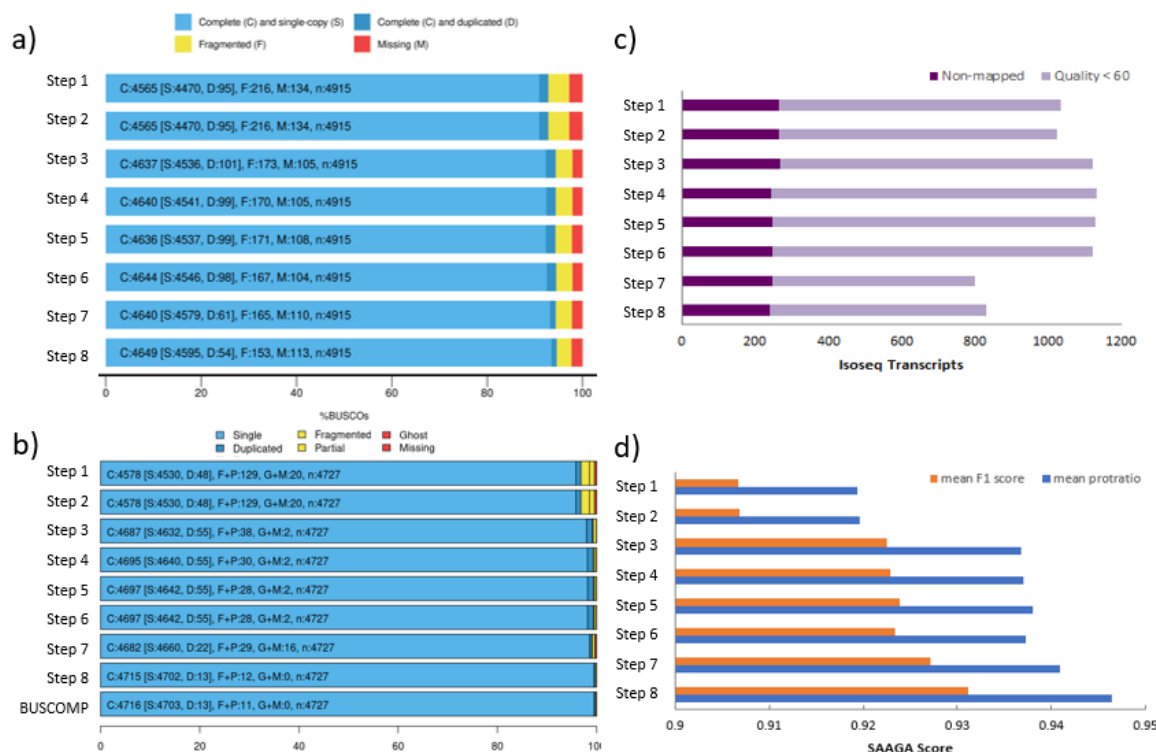
421 Polishing caused a minimal improvement on the total number of mapped Iso-Seq reads, and
422 none were lost during scaffold clean-up with DIPLODOCUS (runmode purgehaplotig and
423 vecscreen). Assessment using GEMoMA and SAAGA revealed that across these assembly
424 steps we see a generally consistent increase in the quality of the predicted proteins during
425 annotation (Fig. 2c), with the largest increases occurring post long-read scaffolding, followed
426 by chromosome scaffolding, and then scaffold clean-up.

427 Of the 33,454 high-quality isoform transcripts in the PacBio Iso-Seq data, only 241
428 failed to map to the final genome assembly, a 17.2% decrease compared to the 291 that failed
429 to map to *S. vulgaris* vNA (Fig. 3b).

430 ***Final genome assembly size, heterozygosity, and contiguity***

431 The *S. vulgaris* vAU assembly of 1,049,838,585 bp covers approximately 93.78% of
432 the total estimated 1.119 Gb genome size (Supplementary Materials: Appendix 2 Validation
433 of SUPERNOVA genome size prediction using JELLYFISH). A similar estimation of genome
434 completeness was reported by K-MER ANALYSIS TOOLKIT (KAT), with the raw read1s (forward
435 reads) estimating a genome completeness of 96.7% (estimated genome size 1.125 Gb,
436 estimated heterozygosity rate 0.57%) and read2s (reverse reads) estimating a genome
437 completeness of 95.92% (estimated genome size 1.135 Gb, estimated heterozygosity rate
438 0.54%) (Supplementary Materials: Fig. S5). Predicted genome sizes based on either read1s or
439 read2s using KAT were slightly larger than the estimation generated by JELLYFISH using all the
440 read data, however the length range was relatively consistent (1.119-1.135 Gb). This
441 assembly reports a scaffold N50 of 72.5 Mb and L50 of 5, with a total of 1,628 scaffolds
442 (Table 2); 98.6% (1,035,260,756 bp) of the sequence length has been assigned to the 32
443 putative nuclear chromosomes (identified via the *T. guttata* v3.2.4 assembly), plus a
444 mitochondrial genome. The final assembly contains 14 macrochromosomes (> 20 Mb, as

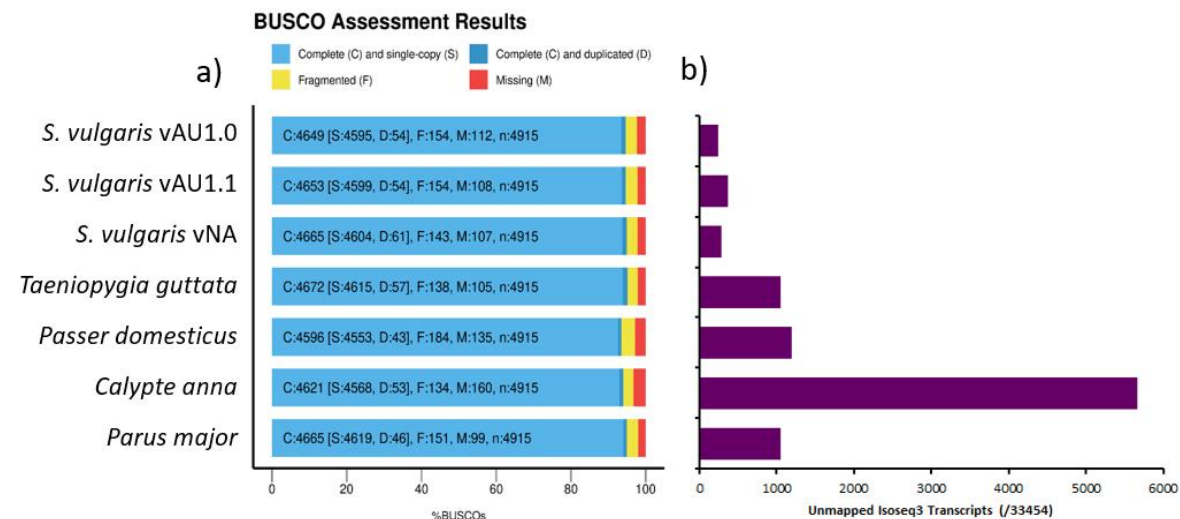
445 described in Backström et al., 2010), with relative sizes appearing in consensus with known
 446 karyotype of *S. vulgaris* (Calafati & Capanna 1981). Macrochromosome scaffolds account for
 447 81.9% of the total assembly size, with the remainder on microchromosomes (16.9%) or
 448 unplaced scaffolds. While these large scaffolds remain only putative chromosomes assuming
 449 karyotype orthology until they can be validated with further read data, increased completeness
 450 scores post chromosomal alignment across all assembly assessment metrics (Fig. 2) support
 451 the assembly structure.



452
 453 **Figure 2: *Sturnus vulgaris* vAU assembly steps overview.** Quality and completeness
 454 assessments for eight sequential assembly steps: step 1 (SUPERNOVA assembly), step 2
 455 (DIPLODOCUS primary assembly), step 3 (SSPACE-LONGREADS scaffolding), step 4
 456 (GAPFINISHER gapfilling), step 5 (L_RNA_SCAFFOLDER), step 6 (PILON polishing), step 7
 457 (DIPLODOCUS clean up), and step 8 (SATSUMA2 Chromosome scaffolding). **a)** BUSCO (Aves,
 458 n=4,915) completeness rating summaries for the sequential steps of *S. vulgaris* genome
 459 assembly. **b)** BUSCOMP completeness results for the 4,727 BUSCO genes identified as
 460 single copy and complete in one or more assembly stages. The final BUSCOMP row
 461 compiles the best rating for each gene across all eight steps. **c)** The number of Iso-Seq reads
 462 that failed to map to each assembly step. **d)** SAAGA annotation scores of mean protein length
 463 ratio (blue) and F1 score (orange) (see Methods for details).
 464

465 **Table 2: *Sturnus vulgaris* overview of assembly statistics** for vAU1.0, vAU1.1, and vNA,
 466 assessed using BUSCOMP.

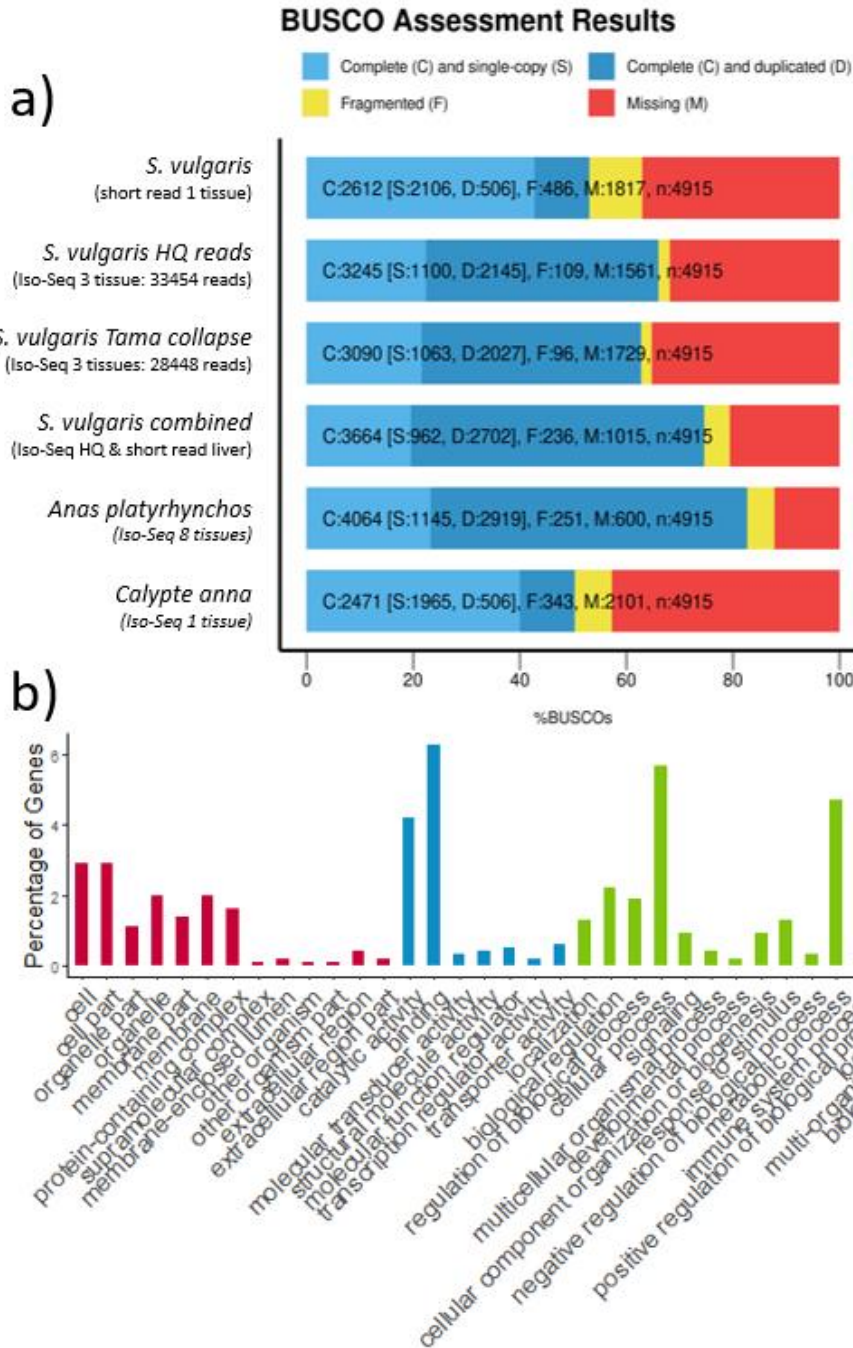
	<i>Sturnus vulgaris</i> vAU1.0	<i>Sturnus vulgaris</i> vAU1.1	<i>Sturnus vulgaris</i> vNA
Total length (bp)	1,049,838,585	1,043,825,671	1,036,755,994
Number of scaffolds	1,628	1,344	2,361
Scaffold N50 (bp)	72,525,610	72,244,370	3,416,708
Scaffold L50	5	5	89
Largest scaffold (bp)	151,927,750	151,503,485	11,828,398
Mean scaffold length (bp)	644,864.0	776,656.01	439,117.3
Median scaffold length (bp)	1,337	1,343	4,856
Number of Contigs	23,815	23,340	22,666
Contig N50 (bp)	145,864	147,322	147,183
Contig L50	2,030	2,010	1,908
Gap (N) length (bp)	13,242,113 (1.26%)	0.74%	23,939,528 (2.31%)
GC (Guanine-Cytosine) content (%)	41.73%	41.72%	41.49%



467
 468 **Figure 3: Assessment of *Sturnus vulgaris* and comparison avian reference assemblies. a)**
 469 BUSCO (Aves) assessments of assembly completeness of *S. vulgaris* vAU1.0, and the NCBI
 470 uploaded genome *S. vulgaris* vAU1.1, presented alongside *S. vulgaris* vNA and four recent
 471 high-quality avian reference genomes (*Taeniopygia guttata* assembly accession
 472 GCF_008822105.2, *Passer domesticus* assembly accession GCA_001700915.1, *Calypte*
 473 *anna* assembly accession GCA_003957555.2, *Parus major* assembly accession
 474 GCA_001522545.3). **b)** Total number of Iso-Seq transcripts that failed to map to each
 475 assembly.

476 **3.2 *Sturnus vulgaris* vAU whole transcriptome data analysis**

477 We generated approximately 68 Gb of PacBio Iso-Seq whole transcript (39,544,054
478 subreads) (Table 1). This produced a total of 33,454 clustered high-quality (predicted
479 accuracy ≥ 0.99) reads, and 157 clustered low-quality (predicted accuracy < 0.99) reads
480 (Supplementary Materials: Table S4). These high-quality read data were used to improve the
481 scaffold assembly of the genome using L_RNA_SCAFFOLDER (see section 2.1) and assess
482 genome completeness (using count comparison of unmapped Iso-Seq reads, see section
483 2.5.2). After being passed through the TAMA *collapse* pipeline, a total of 28,448 non-
484 redundant transcripts were retained to create the final *S. vulgaris* vAU transcriptome, which
485 was used for gene prediction when completing the annotation of the genome assembly. This
486 final three tissue (brain, gonad, heart) Iso-Seq transcriptome had a moderate level overall
487 BUSCO completeness of around 63% that compares to other avian Iso-Seq transcriptomes
488 (Fig. 4a), with a wide range of gene ontology terms identified in the final Iso-Seq transcript
489 list (Fig. 4b) that resembled other avian Iso-Seq GO term distributions (Yin et al., 2019).



490
491
492
493
494
495
496
497
498
499
500

Figure 4: Assessment of 3 tissue Iso-Seq (brain, gonad, heart) *Sturnus vulgaris* transcriptome. a) BUSCO (aves) rating summaries for *S. vulgaris* short read liver transcriptome, the high-quality Iso-Seq *S. vulgaris* transcript produced through the Iso-Seq v3.3 pipeline, the final *S. vulgaris* transcriptome produced by TAMA collapse pipeline, and combined high-quality Iso-Seq and short read liver transcripts, alongside two other avian Iso-Seq transcriptomes (*Anas platyrhynchos* using pectoralis, heart, uterus, ovary, testis, hypothalamus, pituitary and 13 days-old embryo tissue (Yin et al., 2019), and *Calypte anna* using liver tissue (Workman et al., 2018)). b) Breakdown of major GO terms in the sequenced Iso-Seq reads, with Cellular Component (red) Molecular Function (blue) and Biological Process (green).

501 **3.3 *Sturnus vulgaris* genome annotation**

502 The initial annotation produced by GEMOMA, informed by the 26 avian genome
503 annotations available at the time on Ensembl (Supplementary Materials, Table S1), predicted
504 21,539 protein coding genes, with 97.2% BUSCO completeness (93.1% complete when
505 longest protein-per-gene extracted with SAAGA) (Fig. 5). The initial MAKER2 annotation
506 reported 13,495 genes, and a BUSCO completeness of 79.5% (Fig. 5). The merged final
507 annotation reported a BUSCO completeness of 98.2% (Fig. 5a), and this annotation predicted
508 a total of 21,863 protein-coding genes and 79,359 mRNAs. There was an average of 10.7
509 exons and 9.7 introns per mRNA, with an average intron length of 3,364 (Table 3). Of these,
510 1,764 are single-exon genes and 2,330 single-exon mRNA. Predicted coding sequences make
511 up 5.4% of the assembly, with 44.77% remaining outside any gene annotation (Fig. 5b).

512 The predicted transcripts were mapped using SAAGA to the Swiss-Prot database, with
513 66,890 transcripts returning successful hits (84.3%) and 12,469 transcripts remaining
514 unknown (15.7%) for the final annotation (Fig. 6a). The known proteins had an average
515 length of 652 amino acids (aa) and the unknown proteins had an average length of 426 aa
516 (Fig. 6a). Most of the predicted proteins were of high quality, with around 56% of them
517 having an F1 score (see Methods) of greater than 0.95 (Fig. 6b). Similar results were seen
518 when the *Gallus gallus* reference proteome was used, with 69,714 known proteins of average
519 length of 646 aa, 9,645 known proteins of average length of 401 aa, and the final merged
520 annotation having the same F1 score distribution (Fig 6c & 6d).

521 The GEMOMA annotation had similar protein quality patterns, with 57,026 known
522 proteins (average length 664 aa), and 10,400 unknown proteins (average length 401 aa) (Fig.
523 6e). The MAKER2 displayed much greater similarity in protein length histogram between
524 known and unknown proteins, with shorter proteins with known homologs (average length

525 565 aa), but longer unknown proteins (average length 549 aa) (Fig. 6f). The *S. vulgaris* vNA
526 annotation final merged annotation had extremely similar statistics to the final *S. vulgaris*
527 vAU annotation, with an average known protein length of 650 aa, and an average unknown
528 protein length of 407 aa (Supplementary Materials: Figure S2b).

529 **3.4 *Sturnus vulgaris* genome-wide patterns of genomics features**

530 Transcript density compared between mapped Iso-Seq reads and predicted transcripts
531 in the final annotation displayed similar patterns, with some minor variation in patterns
532 between the two tracks (Fig. 7; track 1). Final predicted gene densities (Fig. 7; track 2) were
533 largely following the patterns seen in transcript densities. Further, patterns of transcript and
534 gene numbers across the genome track relatively consistently to GC content (Fig. 7; track 4).

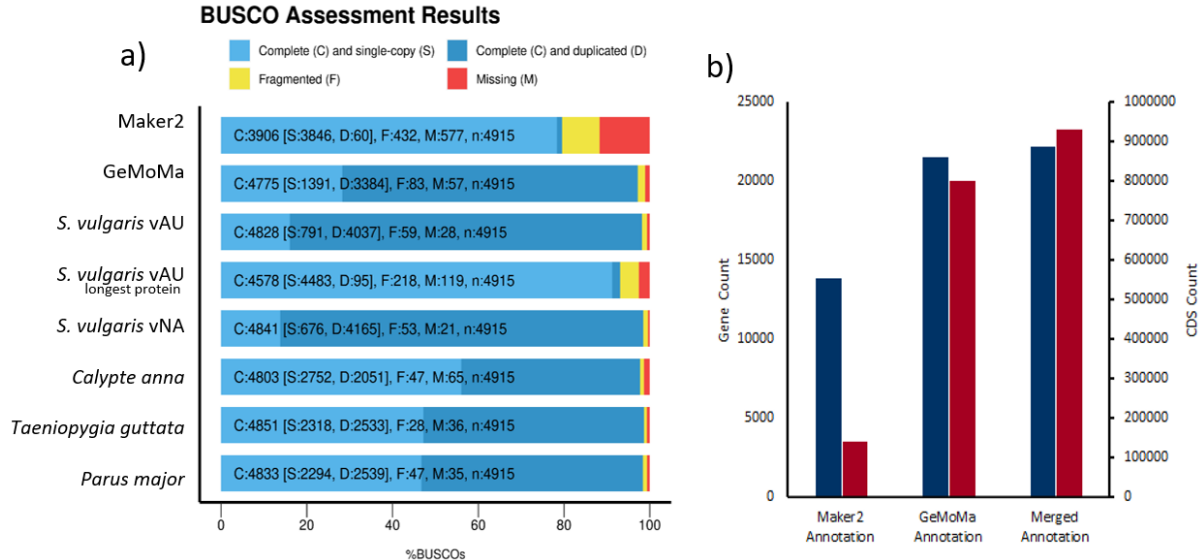
535 Global whole genome variant data (Fig. 7; track 3) revealed genomic regions where
536 variant density is low or non-existent, indicative of high genetic conservation across the
537 species, and genomic regions where variant density peaks are indicative of variant hotspots.
538 Interestingly, we see regions of high conservation corresponding to peaks in gene and/or
539 transcript numbers (e.g., midway through chromosome 4), which may be indicative of regions
540 of highly conserved genes and possibly centromere locations.

541
542
543
544
545
546
547
548
549
550
551

552 **Table 3: Summary of genome annotation of *Sturnus vulgaris* vAU and vNA assemblies.**
553 Statistics extracted using AGAT *agat_sp_functional_statistics.pl*.
554

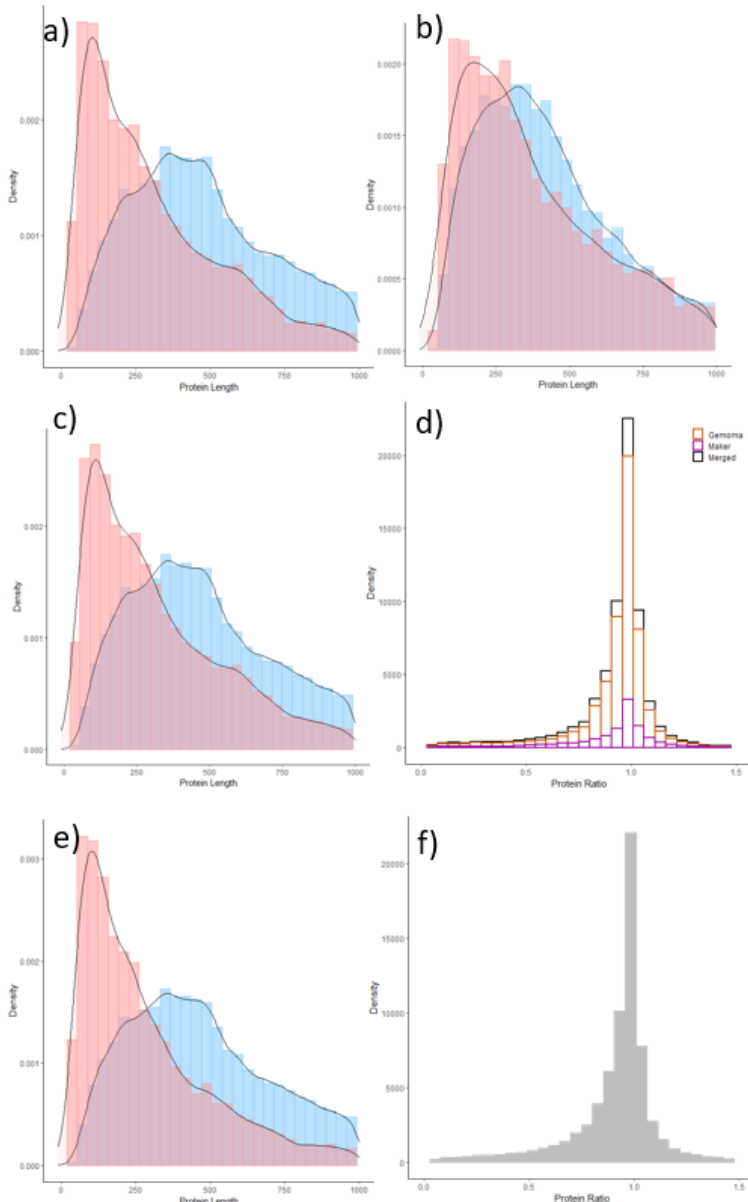
Genome Annotation		<i>S. vulgaris</i> vAU	<i>S. vulgaris</i> vNA
Genes	Total number	21,863	21,944
	Average length	34,699 bp	35,761 bp
	mean mRNAs per gene	3.6	3.7
mRNA	Total number	79,359	81,714
	Average length	38,073 bp	37,857 bp
	mean exons per mRNA	11.8	11.8
CDS	Total number	79,359	81,714
	Average length	1,851	1,836
	Average intron in CDS	3,364	3,343
	length		
Exons	Total number	933,014	962,220
	Mean length	163	158
Gene Function	Ontology Term	60.26% (13174/21863)	59.68% (13097/21944)
	InterPro	78.87% (17244/21863)	77.57% (17022/21944)
	SUPERFAMILY	60.36% (13197/21863)	58.26% (12786/21944)

555
556
557
558
559
560



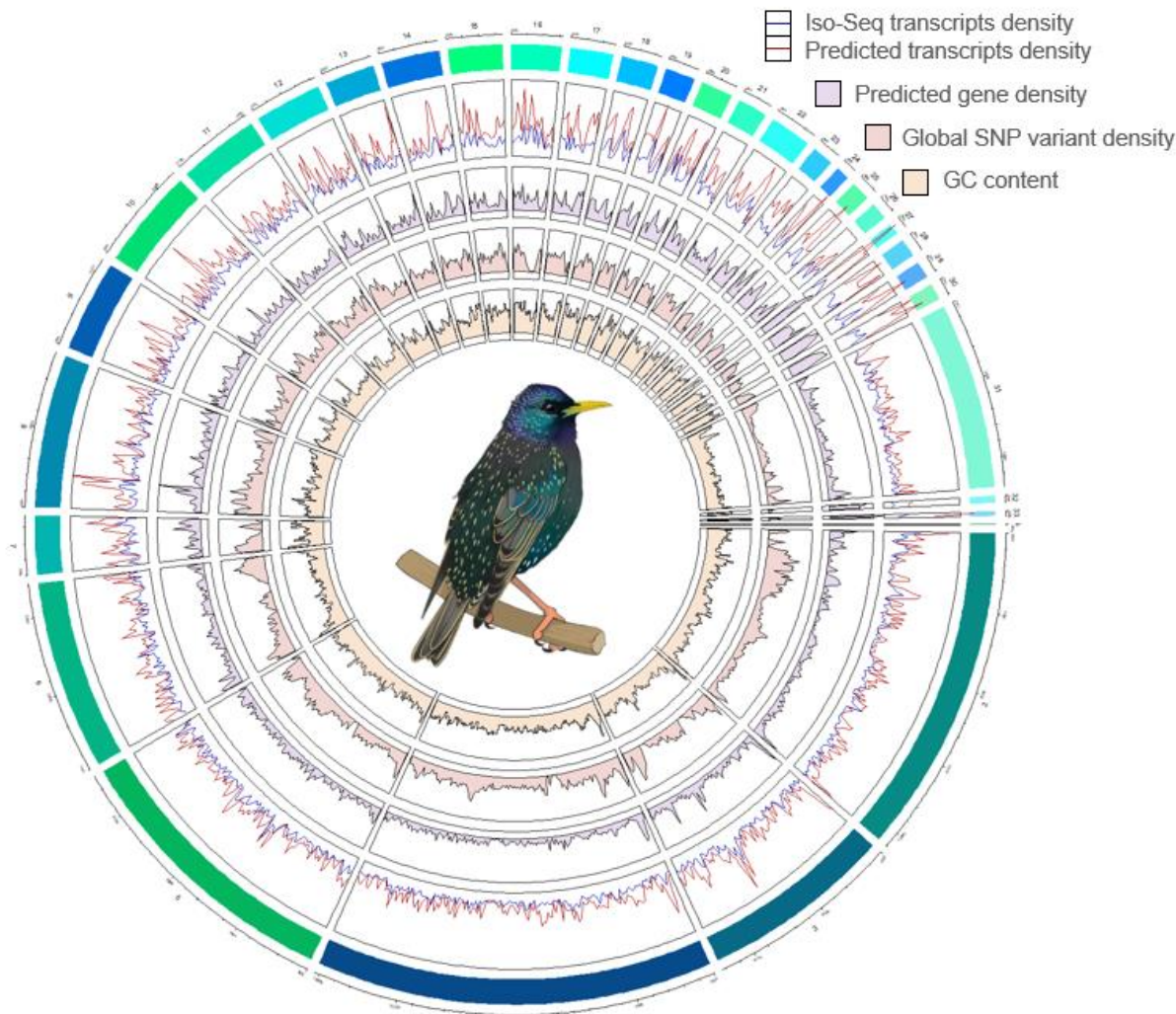
561
562
563
564
565
566
567
568

Figure 5: *Sturnus vulgaris* assessment of annotation. a) BUSCO (Aves) assessments of initial MAKER2 and GEMOMA assemblies, the final *S. vulgaris* vAU annotation, the final annotation with the longest protein-per-gene extracted using SAAGA, the final *S. vulgaris* vNA annotation (combined GEMOMA and MAKER2 annotation), and the ensemble annotations of three additional passerines. **b)** The number of genes (blue) and CDS (red) in the MAKER2 annotation, GEMOMA annotation, and merged annotation.



569

570 **Figure 6: Summary of predicted annotated proteins.** **a)** Protein lengths for known proteins
571 (blue, with a located Swiss-Prot comparison) and unknown proteins (red, those that did not
572 map to Swiss-Prot) for the GEMOMA annotation compared to Swiss-Prot. **b)** Protein lengths
573 of known and unknown proteins for the MAKER2 annotation compared to Swiss-Prot. **c)**
574 Protein lengths of known and unknown proteins for the merged GEMOMA and MAKER2
575 annotation compared to Swiss-Prot. **d)** Protein length ratio between output from SAAGA for
576 all known Swiss-Prot proteins (where a score close to 1 indicates a high-quality gene
577 annotation, protein length ratio calculated as annotated protein length / best Swiss-Prot
578 reference protein length) (merged annotation = black, GEMOMA annotation = orange,
579 MAKER2 annotation = purple). **e)** Protein lengths of known and unknown proteins for the
580 merged GEMOMA and MAKER2 annotation compared to *Gallus gallus* reference proteome
581 (UP000000539_9031). **f)** Protein length ratio between output from SAAGA for the merged
582 annotation against the *Gallus gallus* reference proteome.
583



584

585 **Figure 7: CIRCLIZE plot of the 33 main chromosomal scaffolds** (32 putative autosomes
586 plus mtDNA) in the *Sturnus vulgaris* (*S. vulgaris* vAU) genome assembly (>98% of the total
587 assembly length). The tracks denote variable values in 1,000,000 bp sliding windows. From
588 the outermost track in, the variables displayed are track 1 (Iso-Seq transcripts as blue line,
589 final annotation transcripts as red line), track 2 (final annotation gene counts, purple area),
590 track 3 (variant density, red area), and track 4 GC content (yellow area).

591

592

593

594

595

596

597

598

599

600

601

602 **3.5 BUSCO versus BUSCOMP performance benchmarking**

603 For the non-redundant pseudodiploid *S. vulgaris* vAU SUPERNOVA assembly,
604 BUSCOMP revealed differences in the BUSCO ratings of scaffolds dependent on the
605 assembly background (Fig. 8). Despite the primary ('pri') assembly being a subset of the non-
606 redundant pseudodiploid ('dipnr') assembly, it identified more "Complete" BUSCO genes
607 (4,565 versus 4,532) with fewer "Missing" (131 versus 171) (Fig. 8a). The alternative
608 assembly ('alt') subset similarly returned a partially overlapping set of BUSCO genes with
609 'dipnr', including some not found in 'dipnr' or 'pri': in total, only 101 genes were missing
610 from all three assemblies. Reducing the primary assembly to the 968 (of 18,439) scaffolds
611 containing a complete BUSCO gene ('pribusco'), increased the number of complete genes
612 from 4,565 to 4,586 and reduced the number missing from 131 to 112. Most unexpectedly,
613 reverse complementing these scaffolds reduced the number of BUSCO genes rated
614 "Complete" by two, and increased the number "Missing" by fifteen (Fig. 8a). All five
615 assemblies returned complete BUSCO genes that were fragmented or missing in all the other
616 four assemblies (Supplementary File 1, BUSCOMP v3 results), for a combined total of 4,760
617 complete and only 74 missing.

618 Adding direct or reverse-complemented copies of the 'pribusco' scaffolds increased
619 the number of "Duplicated" genes, but still returned single copy complete genes (Fig. 8b).
620 Doubling and then tripling the assembly size also increased the number of "Missing" genes
621 from 112 to 198 ('duplicate') and then 207 ('triplicate'). As before, these summary numbers
622 hide some gene gains as well as gene losses; only 77 genes are missing from all three BUSCO
623 runs, with 4,750 returned as complete by at least one. Adding randomly shuffled versions of
624 the 'pribusco' scaffolds only had a marginal effect on BUSCO ratings, with four ('2n') to five
625 ('3n', '4n') fewer complete genes returned and seven additional genes missing following

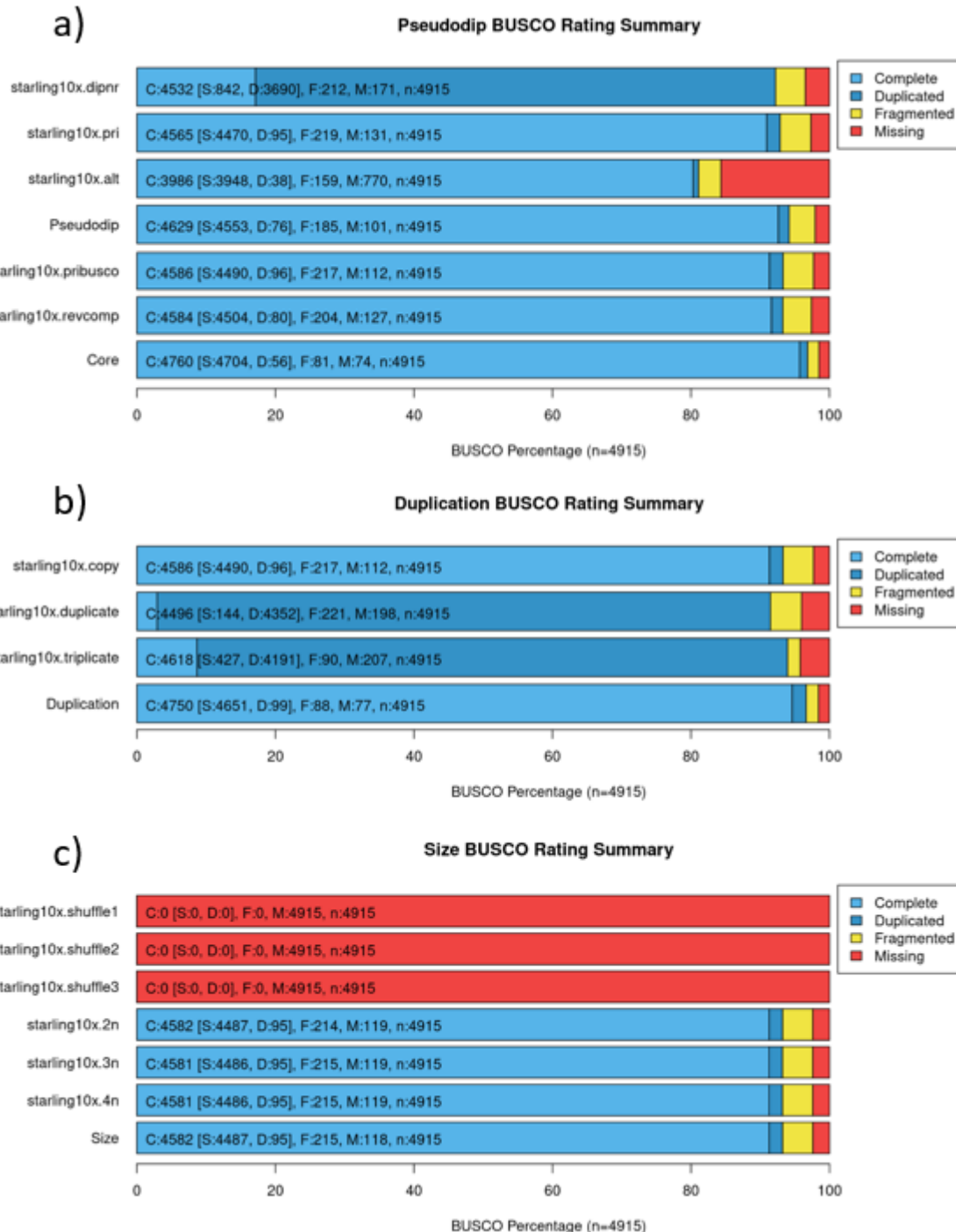
626 addition of the random sequences (Fig. 8c). Ten replicate analyses of the `pribusco` scaffolds
627 returned identical results (Supplementary File 1, BUSCOMP v3 results).

628 In contrast, BUSCOMP completeness is much more consistent across all datasets,
629 with the primary assembly returning the same numbers of complete, partial/fragmented and
630 missing genes as the pseudodiploid assembly (Supplementary File 1, BUSCOMP v3 results).

631 Similarly, reverse complementing scaffolds or increasing genome size gives no difference to
632 the completion statistics. Unlike BUSCO, BUSCOMP rates 100% of complete BUSCO genes
633 for duplicated or triplicated scaffolds as ‘Duplicate’ rather than ‘Single Copy’. Most
634 reassuringly, every complete BUSCO gene returned by a variant or subset of the
635 pseudodiploid assembly is also returned as ‘Complete’ in the pseudodiploid assembly itself.

636 Results using BUSCO v5 and the updated lineage data were qualitatively the same as v3,
637 showing largely identical trends (Supplementary File 2, BUSCOMP v5 results). The
638 exception is that reverse-complementing scaffolds reduced the complete BUSCO genes by
639 one (7,555 to 7,554) and increased the number missing by one (391 to 392). Curiously, this
640 was not reflected by analysis of the duplicated scaffolds, in which all 7,555 ‘pribusco’
641 complete genes were returned as complete and duplicated. It should be noted that the
642 ‘pribusco’ scaffolds for the v5 analysis are missing a greater proportion of the BUSCOMP-
643 compiled single copy complete BUSCO genes because they were still defined from v3 data.

644



645
646

Figure 8. Compiled BUSCO results for benchmarking data.

647
648
649
650
651
652

653

654 **4. Discussion**

655 Here, we present a high-quality, near-complete reference genome for the European
656 starling, *Sturnus vulgaris* vAU, with chromosome-level scaffolding that assigns 98.6% of the
657 genome assembly length to 32 putative nuclear chromosome scaffolds. We demonstrate the
658 utility of both transcripts and gene annotation in validating *S. vulgaris* vAU assembly
659 processes. BUSCOMP, Iso-Seq transcript, and SAAGA annotation assessment were largely in
660 agreement with one another, though each provided additional fine-scale feedback on assembly
661 improvements achieved by each assembly step. These analyses highlight the benefits of these
662 complementary assessment approaches in ensuring that aspects of genome quality are not
663 sacrificed to improve non-specific assembly quality metrics, such as N50. We also present a
664 second, North American, genome assembly, *S. vulgaris* vNA (GCF_001447265.1). Overall,
665 the *S. vulgaris* vAU assembly improved genome assembly statistics over the *S. vulgaris* vNA
666 genome, with a greater percentage of the estimated 1.119 Gb genome represented (94% vs
667 93%), an increase of scaffold N50 from 3.42 Mb to 72.5 Mb, and a decrease in scaffold L50
668 from 89 to 5. The *S. vulgaris* vNA still has good assembly statistics (Table 2, Table S3) and
669 has a marginally higher BUSCO completeness (Fig. 3a) and BUSCOMP completeness
670 (Supplementary Materials: Fig. S6) of approximately 20 BUSCO sequences. There is
671 increasing recognition of the importance of pan-genomes (genome assemblies that
672 differentiate between genes/regions shared by all members of the species, and dispensable or
673 rare genes/regions) (Hirsch et al., 2014; Sherman & Salzberg 2020), which are essential for
674 many model organisms (Vernikos et al., 2015). Having these two high-quality *de novo*
675 assemblies from different populations will improve future genomic work on the global
676 invasive populations of this species, and facilitate review of structural variation (e.g.,
677 inversions) that may exist across different populations. It should be noted, however, that the

678 final scaffolding step for *S. vulgaris* vAU assumed structural conservation between the
679 starling and zebra finch and thus future synteny analyses may want to use the earlier assembly
680 step.

681 **4.1 BUSCO and BUSCOMP assembly completeness assessment**

682 BUSCO (Simão et al., 2015) is an extremely useful and widely-used used assembly
683 assessment tool, providing information on which conserved lineage specific genes are present,
684 fragmented, or absent from a genome assembly. The program, however, can suffer from
685 inconsistent BUSCO gene identification, where a particularly BUSCO may be dropped from a
686 report due to changes elsewhere in the assembly (Edwards 2019), which can result in under-
687 reporting of assembly completeness (Edwards et al., 2018; Field et al., 2020; Edwards et al.,
688 2021). Here, we confirm this behaviour on benchmarking datasets derived from the *S.*
689 *vulgaris* vAU pseudodiploid 10x linked read assembly (Supplementary Materials: Fig. S3, 8).
690 Adding and removing scaffolds can both alter the BUSCO ratings for “Complete” genes
691 within the unchanged scaffolds (Fig. 8, Supplementary File 1, BUSCOMP v3 results,
692 Supplementary File 2, BUSCOMP v5 results). Many of these changes are likely to be the
693 consequence of changes in score thresholds and/or gene prediction models. However, we also
694 demonstrate some unexpected behaviours that are harder to explain, such as changes to
695 BUSCO gene ratings when scaffolds are reverse complemented (Fig 8a).

696 This unpredictable variability in the identification of BUSCOs across genome
697 assembly versions poses some obvious challenges when trying to compare alternate versions
698 of the same assembly. This is particularly true when trying to interpret small changes in
699 BUSCO ratings as assemblies near completion. In addition, an important feature of BUSCO is
700 that it incorporates sequence quality in the context of the gene prediction models it generates.
701 This is desirable for assessing final assembly quality, but can present problems when

702 comparing early assembly stages, prior to error-correction by “polishing”. BUSCOMP
703 (<https://github.com/slimsuite/buscomp>) is robust to differences in assembly size, base-calling
704 quality, and rates the “completeness potential” of an assembly based on the presence of genes
705 first identified for that species by BUSCO. Here, we used BUSCOMP analysis of sequential
706 assembly steps to gain a more accurate understanding of how assembly decisions affected
707 genome completeness (Fig. 2, Supplementary Materials: Fig. S4). BUSCOMP analysis can
708 then be complemented by other tools, such as KAT (Mapleson et al., 2017), SAAGA
709 (<https://github.com/slimsuite/saaga>), and BUSCO itself to get additional assessment of
710 sequence quality.

711 **4.1. Transcript- and annotation-guided *Sturnus vulgaris* vAU genome assembly**

712 The assembly of the *S. vulgaris* vAU genome was improved by assessing mapped Iso-
713 Seq whole transcripts and quality scores of predicted proteins from homology-based
714 annotation. Mapping of the high-quality Iso-Seq reads proved to be an extremely fast method
715 of assessment (33,454 Iso-seq sequences mapped in <5 mins with 16 CPU cores), while the
716 GEMOMA and SAAGA compute time of 12 hrs per assembly was roughly comparable to
717 BUSCO (approximately 50 CPU hrs per assembly on an average machine), though more
718 computationally intensive (GEMOMA ran for approximately 200 CPU hours per assembly,
719 and SAAGA ran for approximately 8 CPU hours per assembly). Over the eight sequential
720 assembly steps, there was a decrease in unmapped Iso-Seq reads, indicating improved
721 sequence representation, with gap-filling yielding the greatest change. Similarly, the quality
722 of annotated proteins predicted by GEMOMA, as assessed by SAAGA, demonstrated ongoing
723 improvements through ONT scaffolding, clean-up, and chromosome alignment. It is also
724 noteworthy that increases in large-scale sequence connectivity using the *T. guttata* genome
725 (Peona et al., 2018) improved the assembly’s performance across all metrics, including

726 completeness estimates, although future Hi-C analysis will be required to confirm the
727 predicted genome structure.

728 Further, BUSCOMP provided an important means of standardising BUSCO
729 annotation ratings across the multiple assembly steps. This method, together with the mapped
730 Iso-Seq reads, can deal with the unpolished intermediary genome steps, and does not suffer
731 the same sequence identification accuracy issues as the traditional stand-alone BUSCO
732 analysis. Together, the standardised assessment reported by BUSCOMP, and the
733 comprehensive and genome/species specific set of genes provided by Iso-seq and
734 GEMOMA/SAAGA showcase the complementary features of these annotation approaches for
735 assembly assessment.

736 **4.2. Improvements to contiguity and completeness during *Sturnus vulgaris* vAU genome
737 assembly**

738 Several alternative assembly pipelines were assessed (Supplementary Materials: Fig.
739 S2), with upstream assembly decisions based primarily on establishing reasonable base
740 assembly statistics (scaffold N50, scaffold L50, contig numbers). Assembly size increased
741 during scaffolding steps, due to estimated bases in gaps, while a decrease in assembly size
742 was only seen during scaffold clean up using *Purgehaplotigs*. Of all the scaffolding steps,
743 scaffolding with the low coverage ONT long reads resulted in the greatest decrease of
744 scaffold L50 (146 scaffold to 39 scaffold, Supplementary Materials: Fig. S4d) and total
745 scaffold number (18,439 scaffolds to 7,856 scaffolds, Supplementary Materials: Fig. S4a). It
746 has previously been shown that even low coverage of ONT data in conjunction with 10x may
747 produce high-quality genome assemblies (Ma et al., 2019). This was true for our data, which
748 demonstrates the utility of even low coverage, long read sequencing (approximately 4.5%
749 coverage based on the estimated genome size of 1.119 Gb) in greatly improving the

750 contiguity of scaffolds generated by short read genome assemblers (though Hi-C data may
751 serve this purpose at a lower cost to scaffold ratio and may assist in identifying
752 misassemblies, which is often not a focus of long-read scaffolding tools). While additional
753 scaffolding using the Iso-Seq whole transcripts did not result in a large increase in continuity
754 (Supplementary Materials: Fig. S4), the Iso-Seq reads were nevertheless were able to scaffold
755 some sequences that failed low coverage ONT scaffolding, reducing the total scaffold count
756 by approximately 100 (7,856 scaffold to 7,776 scaffolds, Supplementary Materials: Fig. S4a).
757 This long-read transcript scaffolding served to minimise the number of fragmented genes in
758 the final assembly, helping downstream analysis and gene prediction models. The final
759 assembly maintained reasonably short contig N50 and high contig L50, which will only be
760 improved with much more extensive long-read sequencing of the species. Nevertheless,
761 scaffolding the *S. vulgaris* genome against that of *T. guttata* was able to further scaffold the
762 genome to a predicted chromosome level, assigning 98.6% of the assembly to previously
763 characterised chromosomes. In support of the assumed synteny of this step, we saw small
764 increases in assembly quality and completeness metrics.

765 The final two assembly steps (contig clean up and chromosomal alignment) were
766 primarily guided by high BUSCO scores and low missing Iso-Seq transcripts (Supplementary
767 Materials: Figure S3). DIPLOIDOCUS *vecscren* did not flag any contamination and so did not
768 result in any assembly decreases. Over-pruning of contigs during clean up (using
769 DIPLOIDOCUS *DipCycle* which is stricter than just *Purgehaplotigs*) resulted in too many
770 (>1,000) discarded scaffolds that decreased assembly completeness scores, most likely
771 because of low coverage ONT long read data. While this drastically improved assembly
772 statistics, this came at the cost of dropped BUSCO sequences. Lastly, assembly duplication
773 analysis using KAT agreed with BUSCO results, indicating there was little final assembly

774 sequence duplication when comparing to raw read k-mer counts (Supplementary Materials:
775 Fig. S5).

776 **4.3. *Sturnus vulgaris* vAU transcriptome**

777 When comparing the completeness of this new starling transcriptome data to existing
778 Illumina short read transcript data produced using liver tissue (Richardson et al., 2017), we
779 see an increase of about 20% in BUSCO completeness, with a particularly large increase in
780 the number of duplicated BUSCO, a result of the alternate transcript isoforms captured
781 through the Iso-Seq. Assessing the effect the TAMA pipeline had on BUSCO completeness,
782 we see a small drop in complete BUSCOs (Fig. 2a) that appear to have been lost during the
783 mapping to genome assembly step. Finally, comparing our final transcriptome to two other
784 avian Iso-Seq transcriptomes gives an indication of how much unique transcript information
785 is added by the addition of tissues into pooled Iso-Seq sequencing runs. The single tissue Iso-
786 Seq liver transcriptome of *Calypte anna* (Anna's hummingbird) (Workman et al., 2018)
787 reported similar BUSCO completeness to the short read *S. vulgaris* liver transcriptome. The
788 eight tissue Iso-Seq transcriptome of *Anas platyrhynchos* (mallard) (Yin et al., 2019) yielded
789 an increase of 30% in complete BUSCOs, consistent with the expectation that our three-tissue
790 Iso-Seq library will be missing a number of tissue-specific genes.

791 **4.4. *Sturnus vulgaris* genome annotation**

792 Of the approximately 22,000 genes reported in the final annotation, 65% were from
793 GEMOMA, and 35% from MAKER2, with the source being randomly selected for common
794 annotation. MAKER2 predicted a higher number of genes in *S. vulgaris* vNA versus *S. vulgaris*
795 vAU (15,150 vs 13,495), while GEMOMA predicted a higher number of genes in the *S.*
796 *vulgaris* vAU genome (21,539 vs 20,414). The ratio in predicted MAKER2 and GEMOMA was
797 more biased towards the homology-based predictor, with an approximate ratio of 1:5 between

798 MAKER2 and GEMOMA (Fig. 5b). Merging of the MAKER2 annotation to the GEMOMA
799 annotation resulted in an increase in 1.1% in BUSCO completeness. Duplication levels were
800 much higher in the GEMOMA annotation when compared to MAKER2 (Fig. 5a). This is not
801 unreasonable, as the GEMOMA annotation will be biased toward well-characterised genes and
802 so may contain more transcripts per gene (Fig. 5b), whereas MAKER2 will inform the
803 prediction of more taxon or possibly species-specific coding sequences. High congruence
804 between Iso-Seq and predicted transcript numbers indicate regions of accurate annotation
805 predictions (Fig. 7). In contrast, Iso-Seq transcripts that are dissimilar or much lower to the
806 predicted transcript densities, are either genomics regions producing tissue specific transcripts
807 not captured by their brain, testes, or muscle, or more likely annotated transcript
808 overprediction.

809 For the final *S. vulgaris* vAU annotation, the predicted proteins of unknown origin
810 (those that failed to map to Swiss-Prot database or *Gallus gallus* proteome) had a smaller
811 average length than those with known homologs (Fig. 6a & 6c). Similar results were found
812 when this approach was used to assess genes predicted in the *R. marina* genome assembly
813 (Edwards et al., 2018), and are indicative that these ‘unknown’ proteins are fragmented and
814 lower quality predictions that may be due to underlying assembly issues with contiguity or
815 frameshifting indels. The poorer quality could also reflect low stringency MAKER2 gene
816 predictions or homology based GEMOMA annotation of low-quality reference genes. The
817 known proteins predicted by MAKER2 (Fig. 6f) were of apparent lower quality than those
818 reported by GEMOMA as indicated by their shorter lengths and lower protein ratios (Fig. 6e),
819 which may be a result from a combination of incorrect gene predictions, and the high-quality
820 reference homologs inflating quality scores of the GEMOMA annotation in comparison.

821 The known protein lengths were similar across the *S. vulgaris* vAU and vNA annotations (652
822 vs 650 aa), though there was a slightly larger difference in average unknown protein length
823 (426 vs 407 aa). Although this increase in *S. vulgaris* vAU is very slight, it may indicate
824 increased quality of unknown protein predictions in the vAU annotation, possibly due to the
825 more Iso-Seq data mapping to the vAU genome (Fig. 4b) or the higher contiguity. Predicted
826 genes were more commonly shorter than their closest reference protein hits, indicative there
827 might still be some truncated gene predictions, consistent with the large number of assembly
828 gaps. Nevertheless, the final annotation has a strong protein ratio peak around 1.0 for known
829 proteins (Fig. 6b & 6d), indicating that the bulk of these predicted genes were of lengths
830 similar to their Swiss-Prot homologs and hence deemed high quality.

831 Near identical assembly pipelines were used for the annotation of the two genome
832 assemblies, with the resulting final gene count predictions comparable to other high-quality
833 avian genomes and expected gene counts in eukaryote genomes. Both genome assembly
834 versions reported similar final annotation statistics, with *S. vulgaris* vNA reporting slightly
835 more predicted genes (Table 3), and a larger predicted gene coverage over the genome
836 (59.09% gene coverage vs 55.23%), indicating this increase in predicted genes is not just a
837 result of more overlapped predictions, though it could be a result of smaller assembly size and
838 higher gene duplication (Fig. 5a).

839

840 **5. Conclusion:**

841 This paper highlights the multifunctional use of species-specific transcript data, and
842 the importance of diverse assessment tools in the assembly and assessment of reference
843 genomes and annotations. We present a high-quality, annotated *S. vulgaris* vAU reference
844 genome, scaffolded at the chromosome level. Alongside a second assembly, *S. vulgaris* vNA,

845 these data provide vital resources for characterising the diverse and changing genomic
846 landscape of this globally important avian. In addition to improving the completeness of gene
847 annotation, we demonstrate the utility of long-read transcript data for genome quality
848 assessment and assembly scaffolding. We also reveal some counter-intuitive behaviour of
849 BUSCO genome completeness statistics, and present complementary two tools, BUSCOMP
850 and SAAGA, which can identify and resolve potential artefacts, and inform assembly pipeline
851 decisions.

852 **Author Contributions**

853 Project conception: all authors
854 Sample Collection: KCS, SJW, MCB
855 Lab Work: KCS, YC, LAR, WCW
856 Data Analysis: KCS, RJE, YC, WCW
857 Program Development: RJE
858 Manuscript Writing: KCS, RJE
859 Manuscript Editing: All authors

860 **Acknowledgements:**

861 We thank non-author members of the Starling Genome Consortium for their support of this
862 project including Wim Vanden Berghe. Thank you to Stella Loke, Annabel Whibley, and
863 Mark Richardson for their guidance of Nanopore sequencing and analysis. Thank you to
864 Daniel Selechnik for assistance with RNA extractions. Art credit (Fig. 7 illustration) to
865 Megan Bishop. RJE was funded by the Australian Research Council (LP160100610 and
866 LP18010072). DWB and YC acknowledge grant funding from the Human Sciences Frontier
867 Programme (Grant RGP0030/2015). SM acknowledges Roslin Institute Strategic Grant
868 funding from the UK Biotechnology and Biological Sciences Research Council

869 (BB/P013759/1). LAR was supported by a Scientia Fellowship from UNSW.

870 **Data Accessibility and Programs**

871 BUSCOMP documentation: <https://slimsuite.github.io/buscomp/>

872 Diploidocus documentation: <https://slimsuite.github.io/diploidocus/>

873 SAAGA documentation: <https://slimsuite.github.io/saaga/>

874 The data have been deposited with links to BioProject accession number PRJNA706841 in
875 the NCBI BioProject database (<https://www.ncbi.nlm.nih.gov/bioproject/>). Bioproject raw
876 data reviewer link is available at:

877 <https://dataview.ncbi.nlm.nih.gov/object/PRJNA706841?reviewer=op1k3u6792jbg8o4rddq138g9e>

879 Genome accession JAGFZL000000000 is currently private on NCBI, but a reviewer copy is
880 available here: <https://drive.google.com/drive/folders/1MTEExtlui-I-ziCIzwyBtgiP0NwHTg3IG?usp=sharing>

882 Any scripts or metadata not covered by the above will be available on GitHub.

883 **References:**

884 Backström N, Forstmeier W, Schielzeth H, Mellenius H, Nam K, Bolund E, Webster MT, Öst T,
885 Schneider M, Kempenaers B *et al.* 2010 The recombination landscape of the zebra finch
886 *Taeniopygia guttata* genome. *Genome Research* **20** 485–495. (doi:10.1101/gr.101410.109)

887 Balakrishnan CN, Edwards SV & Clayton DF 2010 The Zebra Finch genome and avian genomics in the
888 wild. *Emu - Austral Ornithology* **110** 233–241. (doi:10.1071/MU09087)

889 Bateson M & Feenders G 2010 The use of passerine bird species in laboratory research: implications
890 of basic biology for husbandry and welfare. *ILAR Journal* **51** 394–408.
891 (doi:10.1093/ilar.51.4.394)

892 BirdLife International 2020 Species factsheet: *Sturnus vulgaris*. In *BirdLife International*.

893 Bodt LH, Rollins LA & Zichello J 2020 Genetic Diversity of the European Starling (*Sturnus vulgaris*)
894 Compared Across Three Invasive Ranges.

895 Boetzer M & Pirovano W 2014 SSPACE-LongRead: scaffolding bacterial draft genomes using long read
896 sequence information. *BMC Bioinformatics* **15** 211. (doi:10.1186/1471-2105-15-211)

897 Bomford M & Sinclair R 2002 Australian research on bird pests: impact, management and future
898 directions. *Emu - Austral Ornithology* **102** 29–45. (doi:10.1071/MU01028)

899 Bradnam KR, Fass JN, Alexandrov A, Baranay P, Bechner M, Birol I, Boisvert S, Chapman JA, Chapuis
900 G, Chikhi R *et al.* 2013 Assemblathon 2: evaluating de novo methods of genome assembly in
901 three vertebrate species. *GigaScience* **2**. (doi:10.1186/2047-217X-2-10)

902 Calafati P & Capanna E 1981 Karyotype analysis in ornithological studies: the chromosomes of six
903 species of oscines (passeriformes). *Avocetta* **5** 1–5.

904 Camacho C, Coulouris G, Avagyan V, Ma N, Papadopoulos J, Bealer K & Madden TL 2009 BLAST+:
905 architecture and applications. *BMC Bioinformatics* **10** 421. (doi:10.1186/1471-2105-10-421)

906 Coleman JD 1977 The foods and feeding of starlings in Canterbury. *Proceedings (New Zealand*
907 *Ecological Society)* **24** 94–109.

908 Davey NE, Shields DC & Edwards RJ 2006 SLiMDisc: short, linear motif discovery, correcting for
909 common evolutionary descent. *Nucleic Acids Research* **34** 3546–3554.
910 (doi:10.1093/nar/gkl486)

911 Edwards R 2019 BUSCOMP: BUSCO compilation and comparison – Assessing completeness in
912 multiple genome assemblies. *F1000Research* **8**:995 (slides).
913 (doi:10.7490/f1000research.1116972.1)

914 Edwards RJ, Tuipulotu DE, Amos TG, O'Meally D, Richardson MF, Russell TL, Vallinoto M, Carneiro M,
915 Ferrand N, Wilkins MR *et al.* 2018 Draft genome assembly of the invasive cane toad, *Rhinella*
916 *marina*. *GigaScience* **7**. (doi:10.1093/gigascience/giy095)

917 Edwards RJ, Field MA, Ferguson JM, Dudchenko O, Keilwagen J, Rosen BD, Johnson GS, Rice ES, Hillier
918 LD, Hammond JM *et al.* 2021 Chromosome-length genome assembly and structural
919 variations of the primal Basenji dog (*Canis lupus familiaris*) genome. *BMC Genomics* **22** 188.
920 (doi:10.1186/s12864-021-07493-6)

921 Feare CJ 1985 *The Starling*. Shire.

922 Field MA, Rosen BD, Dudchenko O, Chan EKF, Minoche AE, Edwards RJ, Barton K, Lyons RJ, Tuipulotu
923 DE, Hayes VM *et al.* 2020 Canfam_GSD: De novo chromosome-length genome assembly of
924 the German Shepherd Dog (*Canis lupus familiaris*) using a combination of long reads, optical
925 mapping, and Hi-C. *GigaScience* **9**. (doi:10.1093/gigascience/giaa027)

926 Flynn JM, Hubley R, Goubert C, Rosen J, Clark AG, Feschotte C & Smit AF 2020 RepeatModeler2 for
927 automated genomic discovery of transposable element families. *Proceedings of the National*
928 *Academy of Sciences* **117** 9451–9457. (doi:10.1073/pnas.1921046117)

929 Griffin DK, Robertson LBW, Tempest HG & Skinner BM 2007 The evolution of the avian genome as
930 revealed by comparative molecular cytogenetics. *Cytogenetic and Genome Research* **117** 64–
931 77. (doi:10.1159/000103166)

932 Gs S & E B 2005 Automated generation of heuristics for biological sequence comparison. *BMC*
933 *Bioinformatics* **6** 31–31. (doi:10.1186/1471-2105-6-31)

934 Gu Z, Gu L, Eils R, Schlesner M & Brors B 2014 circlize Implements and enhances circular visualization
935 in R. *Bioinformatics (Oxford, England)* **30** 2811–2812. (doi:10.1093/bioinformatics/btu393)

936 Hirsch CN, Foerster JM, Johnson JM, Sekhon RS, Muttoni G, Vaillancourt B, Peñagaricano F, Lindquist
937 E, Pedraza MA, Barry K *et al.* 2014 Insights into the Maize Pan-Genome and Pan-
938 Transcriptome. *The Plant Cell* **26** 121–135. (doi:10.1105/tpc.113.119982)

939 Hofmeister NR, Werner SJ & Lovette IJ 2019 Environment but not geography explains genetic
940 variation in the invasive and largely panmictic European starling in North America. *BioRxiv*
941 643858. (doi:10.1101/643858)

942 Hofmeister NR, Stuart K, Warren WC, Werner SJ, Bateson M, Ball GF, Buchanan KL, Burt DW, Cardilini
943 APA, Cassey P *et al.* 2021 Concurrent invasions by European starlings (*Sturnus vulgaris*)
944 suggest selection on shared genomic regions even after genetic bottlenecks. *BioRxiv*
945 2021.05.19.442026. (doi:10.1101/2021.05.19.442026)

946 Holt C & Yandell M 2011 MAKER2: an annotation pipeline and genome-database management tool
947 for second-generation genome projects. *BMC Bioinformatics* **12** 491. (doi:10.1186/1471-
948 2105-12-491)

949 Hunt M, Kikuchi T, Sanders M, Newbold C, Berriman M & Otto TD 2013 REAPR: a universal tool for
950 genome assembly evaluation. *Genome Biology* **14** R47. (doi:10.1186/gb-2013-14-5-r47)

951 Hyatt D, Chen G-L, LoCascio PF, Land ML, Larimer FW & Hauser LJ 2010 Prodigal: prokaryotic gene
952 recognition and translation initiation site identification. *BMC Bioinformatics* **11** 119.
953 (doi:10.1186/1471-2105-11-119)

954 Jayakumar V & Sakakibara Y 2019 Comprehensive evaluation of non-hybrid genome assembly tools
955 for third-generation PacBio long-read sequence data. *Briefings in Bioinformatics* **20** 866–876.
956 (doi:10.1093/bib/bbx147)

957 Keilwagen J, Hartung F, Paulini M, Twardziok SO & Grau J 2018 Combining RNA-seq data and
958 homology-based gene prediction for plants, animals and fungi. *BMC Bioinformatics* **19** 189.
959 (doi:10.1186/s12859-018-2203-5)

960 Koch AJ, Munks SA & Spencer C 2009 Bird use of native trees retained in young eucalypt plantations:
961 species richness and use of hollows. *Wildlife Research* **36** 581–591. (doi:10.1071/WR09037)

962 Kono N & Arakawa K 2019 Nanopore sequencing: Review of potential applications in functional
963 genomics. *Development, Growth & Differentiation* **61** 316–326.
964 (doi:<https://doi.org/10.1111/dgd.12608>)

965 Korf I 2004 Gene finding in novel genomes. *BMC Bioinformatics* **5** 59. (doi:10.1186/1471-2105-5-59)

966 Kuo RI, Cheng Y, Zhang R, Brown JWS, Smith J, Archibald AL & Burt DW 2020 Illuminating the dark
967 side of the human transcriptome with long read transcript sequencing. *BMC Genomics* **21**
968 751. (doi:10.1186/s12864-020-07123-7)

969 Levy Karin E, Mirdita M & Söding J 2020 MetaEuk—sensitive, high-throughput gene discovery, and
970 annotation for large-scale eukaryotic metagenomics. *Microbiome* **8** 48. (doi:10.1186/s40168-
971 020-00808-x)

972 Li H 2018 Minimap2: pairwise alignment for nucleotide sequences. *Bioinformatics (Oxford, England)*
973 **34** 3094–3100. (doi:10.1093/bioinformatics/bty191)

974 Linz GM, Homan HJ, Gaulker SM, Penry LB & Bleier WJ 2007 European starlings: A review of an
975 invasive species with far-reaching impacts. *Managing Vertebrate Invasive Species*.

976 Linz G, Johnson R & Thiele J 2017 European Starlings. In *Ecology and Management of Terrestrial*
977 *Vertebrate Invasive Species in the United States*, 1st ed, pp 311–332. Ed WC Pitt. Boca Raton :
978 Taylor & Francis, 2018. | “A CRC title, part of the Taylor & Francis imprint, a member of the
979 Taylor & Francis Group, the academic division of T&F Informa plc.”: CRC Press.
980 (doi:10.1201/9781315157078-15)

981 Ma Z (Sam), Li L, Ye C, Peng M & Zhang Y-P 2019 Hybrid assembly of ultra-long Nanopore reads
982 augmented with 10x-Genomics contigs: Demonstrated with a human genome. *Genomics* **111**
983 1896–1901. (doi:10.1016/j.ygeno.2018.12.013)

984 Mapleson D, Garcia Accinelli G, Kettleborough G, Wright J & Clavijo BJ 2017 KAT: a K-mer analysis
985 toolkit to quality control NGS datasets and genome assemblies. *Bioinformatics* **33** 574–576.
986 (doi:10.1093/bioinformatics/btw663)

987 Marçais G & Kingsford C 2011 A fast, lock-free approach for efficient parallel counting of occurrences
988 of k-mers. *Bioinformatics* **27** 764–770. (doi:10.1093/bioinformatics/btr011)

989 Mirarab S, Nguyen N & Warnow T 2012 SEPP: SATé-enabled phylogenetic placement. *Pacific*
990 *Symposium on Biocomputing. Pacific Symposium on Biocomputing* 247–258.
991 (doi:10.1142/9789814366496_0024)

992 O'Connor RE, Kiazim L, Skinner B, Fonseka G, Joseph S, Jennings R, Larkin DM & Griffin DK 2019
993 Patterns of microchromosome organization remain highly conserved throughout avian
994 evolution. *Chromosoma* **128** 21–29. (doi:10.1007/s00412-018-0685-6)

995 Palacio FX, Maragliano RE & Montalti D 2016 Functional role of the invasive European Starling,
996 *Sturnus vulgaris*, in Argentina. *Emu* **116** 387–393. (doi:10.1071/MU16021)

997 Peona V, Weissensteiner MH & Suh A 2018 How complete are “complete” genome assemblies?—An
998 avian perspective. *Molecular Ecology Resources* **18** 1188–1195.
999 (doi:<https://doi.org/10.1111/1755-0998.12933>)

1000 Phair DJ, Roux JJL, Berthouly-Salazar C, Visser V, Vuuren BJ van, Cardilini APA & Hui C 2018 Context-
1001 dependent spatial sorting of dispersal-related traits in the invasive starlings (*Sturnus vulgaris*)
1002 of South Africa and Australia. *BioRxiv* 342451. (doi:10.1101/342451)

1003 Prentis PJ, Wilson JRU, Dormontt EE, Richardson DM & Lowe AJ 2008 Adaptive evolution in invasive
1004 species. *Trends in Plant Science* **13** 288–294. (doi:10.1016/j.tplants.2008.03.004)

1005 Quinlan AR & Hall IM 2010 BEDTools: a flexible suite of utilities for comparing genomic features.
1006 *Bioinformatics* **26** 841–842. (doi:10.1093/bioinformatics/btq033)

1007 Rhie A, McCarthy SA, Fedrigo O, Damas J, Formenti G, Koren S, Uliano-Silva M, Chow W,
1008 Fungtammasan A, Gedman GL *et al.* 2020 Towards complete and error-free genome
1009 assemblies of all vertebrate species. *BioRxiv* 2020.05.22.110833.
1010 (doi:10.1101/2020.05.22.110833)

1011 Rice P, Longden I & Bleasby A 2000 EMBOSS: the European Molecular Biology Open Software Suite.
1012 *Trends in Genetics: TIG* **16** 276–277. (doi:10.1016/s0168-9525(00)02024-2)

1013 Richardson MF, Sherwin WB & Rollins LA 2017 De Novo Assembly of the Liver Transcriptome of the
1014 European Starling, *Sturnus vulgaris*. *Journal of Genomics* **5** 54–57. (doi:10.7150/jgen.19504)

1015 Rintala J, Tiainen J & Pakkala T 2003 Population trends of the Finnish starling *Sturnus vulgaris*, 1952–
1016 1998, as inferred from annual ringing totals. *Annales Zoologici Fennici* **40** 365–385.

1017 Robinson RA, Siriwardena GM & Crick HQP 2005 Status and population trends of Starling *Sturnus*
1018 *vulgaris* in Great Britain. *Bird Study* **52** 252–260. (doi:10.1080/00063650509461398)

1019 Rosenberg KV, Dokter AM, Blancher PJ, Sauer JR, Smith AC, Smith PA, Stanton JC, Panjabi A, Helft L,
1020 Parr M *et al.* 2019 Decline of the North American avifauna. *Science* **366** 120–124.
1021 (doi:10.1126/science.aaw1313)

1022 Sherman RM & Salzberg SL 2020 Pan-genomics in the human genome era. *Nature Reviews Genetics*
1023 **21** 243–254. (doi:10.1038/s41576-020-0210-7)

1024 Simão FA, Waterhouse RM, Ioannidis P, Kriventseva EV & Zdobnov EM 2015 BUSCO: assessing
1025 genome assembly and annotation completeness with single-copy orthologs. *Bioinformatics*
1026 (*Oxford, England*) **31** 3210–3212. (doi:10.1093/bioinformatics/btv351)

1027 Smit A, Hubley R & Green P 2013 *RepeatMasker Open-4.0*.

1028 Spooner FEB, Pearson RG & Freeman R 2018 Rapid warming is associated with population decline
1029 among terrestrial birds and mammals globally. *Global Change Biology* **24** 4521–4531.
1030 (doi:<https://doi.org/10.1111/gcb.14361>)

1031 Stanke M & Morgenstern B 2005 AUGUSTUS: a web server for gene prediction in eukaryotes that
1032 allows user-defined constraints. *Nucleic Acids Research* **33** W465–W467.
1033 (doi:10.1093/nar/gki458)

1034 Steinegger M & Söding J 2017 MMseqs2 enables sensitive protein sequence searching for the
1035 analysis of massive data sets. *Nature Biotechnology* **35** 1026–1028. (doi:10.1038/nbt.3988)

1036 Stuart KC, Cardilini APA, Cassey P, Richardson MF, Sherwin W, Rollins LA & Sherman CDH 2020
1037 Signatures of selection in a recent invasion reveals adaptive divergence in a highly vagile
1038 invasive species. *Molecular Ecology* **n/a**. (doi:10.1111/mec.15601)

1039 UniProt Consortium 2019 UniProt: a worldwide hub of protein knowledge. *Nucleic Acids Research* **47**
1040 D506–D515. (doi:10.1093/nar/gky1049)

1041 Vernikos G, Medini D, Riley DR & Tettelin H 2015 Ten years of pan-genome analyses. *Current Opinion*
1042 *in Microbiology* **23** 148–154. (doi:10.1016/j.mib.2014.11.016)

1043 Walker BJ, Abeel T, Shea T, Priest M, Abouelliel A, Sakthikumar S, Cuomo CA, Zeng Q, Wortman J,
1044 Young SK *et al.* 2014 Pilon: An Integrated Tool for Comprehensive Microbial Variant
1045 Detection and Genome Assembly Improvement. *PLOS ONE* **9** e112963.
1046 (doi:10.1371/journal.pone.0112963)

1047 Weisenfeld NI, Kumar V, Shah P, Church DM & Jaffe DB 2017 Direct determination of diploid genome
1048 sequences. *Genome Research* **27** 757–767. (doi:10.1101/gr.214874.116)

1049 Wheeler TJ & Eddy SR 2013 nhmmer: DNA homology search with profile HMMs. *Bioinformatics* **29**
1050 2487–2489. (doi:10.1093/bioinformatics/btt403)

1051 Whibley A, Kelley JL & Narum SR 2020 The changing face of genome assemblies: Guidance on
1052 achieving high-quality reference genomes. *Molecular Ecology Resources*. (doi:10.1111/1755-
1053 0998.13312)

1054 Workman RE, Myrka AM, Wong GW, Tseng E, Welch KC & Timp W 2018 Single-molecule, full-length
1055 transcript sequencing provides insight into the extreme metabolism of the ruby-throated
1056 hummingbird *Archilochus colubris*. *GigaScience* **7**. (doi:10.1093/gigascience/giy009)

1057 Wretenberg J, Lindström Å, Svensson S, Thierfelder T & Pärt T 2006 Population trends of farmland
1058 birds in Sweden and England: similar trends but different patterns of agricultural
1059 intensification. *Journal of Applied Ecology* **43** 1110–1120. (doi:10.1111/j.1365-
1060 2664.2006.01216.x)

1061 Xue W, Li J-T, Zhu Y-P, Hou G-Y, Kong X-F, Kuang Y-Y & Sun X-W 2013 L_RNA_scaffolder: scaffolding
1062 genomes with transcripts. *BMC Genomics* **14** 604. (doi:10.1186/1471-2164-14-604)

1063 Ye J, Zhang Y, Cui H, Liu J, Wu Y, Cheng Y, Xu H, Huang X, Li S, Zhou A *et al.* 2018 WEGO 2.0: a web
1064 tool for analyzing and plotting GO annotations, 2018 update. *Nucleic Acids Research* **46**
1065 W71–W75. (doi:10.1093/nar/gky400)

1066 Yin Z, Zhang F, Smith J, Kuo R & Hou Z-C 2019 Full-length transcriptome sequencing from multiple
1067 tissues of duck, *Anas platyrhynchos*. *Scientific Data* **6** 275. (doi:10.1038/s41597-019-0293-1)

1068 Yuan Y, Bayer PE, Scheben A, Chan C-KK & Edwards D 2017 BioNanoAnalyst: a visualisation tool to
1069 assess genome assembly quality using BioNano data. *BMC Bioinformatics* **18** 323.
1070 (doi:10.1186/s12859-017-1735-4)

1071